ARCHIVES OF ACOUSTICS
2, 3, 167-176 (1977)

THE LOCATION OF THE GROUND FOCUS LINE PRODUCED BY A SUPERSONIC AIRCRAFT

RUFIN MAKAREWICZ

Chair of Acoustics, A. Mickiewicz University (Poznań)

An aircraft flying at a speed higher than that of the propagation of sound produces a supersonic boom, and it has been observed that certain changes in the flight velocity or direction are accompanied by focussing the boom. In this paper procedural algorithms are presented which permit determination of the points on the Earth's surface at which this phenomenon occurs, for any manoeuvre (in section 2) and for accelerated rectilinear flight (in section 3).

1. Introduction

An aircraft flying at a supersonic velocity is the source of an acoustic disturbance called a *sonic boom* or *N wave* (Fig. 1).

This wave can be characterized by two parameters: the shock wave pressure jump Δp and the time Δt of its rising. It has been noted (e.g. WANNER [6]) that under certain conditions the value of Δp is very large (of

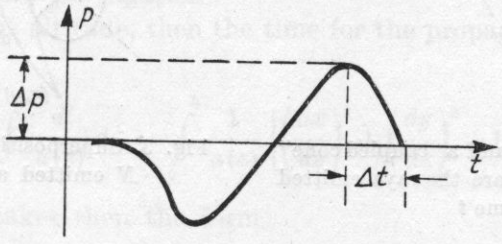

Fig. 1. N wave signature for flight at supersonic speed

the order of tens of kG/m^2). This is caused by the focussing effected by a superposition of sonic booms. The rapid change of sign of Δp (from an excess pressure to a negative pressure — Fig. 1) is liable to cause damage to building-structures and living organisms (including the failure of internal organs).

The problem of localization of the focussing is of importance since although focussing is a hazard for the human environment, it is unavoidable if the benefits of supersonic aircraft are to be exploited. The primary cause of focussing is usually an aircraft manoeuvre, i.e. a change of velocity or flight direction. It is important that this flight manoeuvre (e.g. acceleration to supersonic velocity) should not lead to the focussing of waves on densely populated agglomerations or on recreation and rest areas.

In section 2 of this paper a procedural algorithm is proposed which permits the localization of the focussing region for any aircraft manoeuvre. The starting point for this procedure is the condition that at least two N waves will coincide in space and time. In other papers dealing with this problem (e.g. [2, 6, 7]) the focussing points are identified with the so-called *apex points* and thus tend to obscure the physical meaning of the focussing phenomenon. The algorithm developed for the case of rectilinear accelerated flight (section 3) is much simpler. It is based on a particular effect which occurs during this manoeuvre.

2. Determination of the focussing region in the general case

In the close proximity of the aircraft the sonic bang produces a Mach cone. Each point of the cone's surface can be considered to be the end of a ray emitted from the apex of the cone at an earlier moment (Fig. 2). The set of all rays emitted at any moment forms a "coupled cone" whose generating

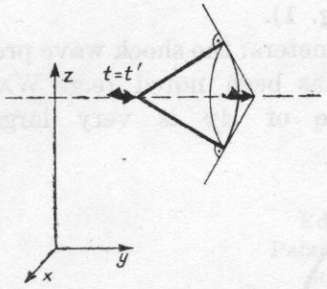

Fig. 2. The Mach cone and a "coupled cone" whose generating lines are the rays emitted at a time t

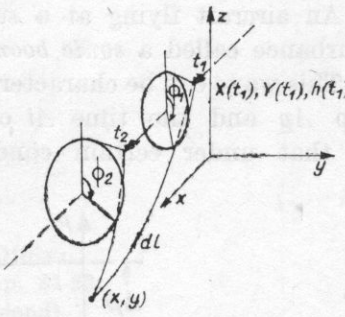

Fig. 3. Superposition (focussing) of waves N emitted at times t_1 and t_2

lines, in the proximity of the aircraft, are perpendicular to the generating lines of the Mach cone. Two such coupled cones are shown in Fig. 3. Owing to refraction, these rays are in fact curves and the surfaces are somewhat distorted.

Focussing of supersonic waves at the point (x, y) will take place when at least two waves reach this point simultaneously. Two rays are marked in Fig. 3 as paths along which the waves are propagated. If we denote the times

of emission of the superimposing waves by t_1 and t_2, and the times of arrival at the point (x, y) by $t^{(1)}$ and $t^{(2)}$, then the following equation must be satisfied:

$$t^{(1)} = (t_2 - t_1) + t^{(2)}. \tag{1}$$

The length of the segment dl (Fig. 3) is

$$dl = \{(dx)^2 + (dy)^2 + (dz)^2\}^{1/2},$$

hence

$$dl = \left\{\left(\frac{dx}{dz}\right)^2 + \left(\frac{dy}{dz}\right)^2 + 1\right\}^{1/2}.$$

For the expressions dx/dz and dy/dz of the acoustic rays in an inhomogeneous medium (derived for example in [1]) we have

$$\begin{aligned} \frac{dx}{dz} &= \frac{[a(z)\cos\theta + W_x(z)]\cos\vartheta}{a(z)\{\cos^2\vartheta - \cos^2\theta\}^{1/2} + W_z(z)\cos\vartheta}, \\ \frac{dy}{dz} &= \frac{[a(z)\cos\theta\tan\vartheta + W_y(z)]\cos\vartheta}{a(z)\{\cos^2\vartheta - \cos^2\theta\}^{1/2} + W_z(z)\cos\vartheta}, \end{aligned} \tag{2}$$

where

$$\vartheta = \gamma + \operatorname{arc\,tan}\left[\operatorname{cotan}\alpha\frac{\sin\Phi}{\cos\delta}\right],$$

$$\cos\theta = \cos\gamma[\cos\delta\sin\alpha - \sin\delta\cos\alpha\cos\Phi] - \sin\gamma\cos\alpha\sin\Phi,$$

with

$$\alpha = \operatorname{arc\,sin}\frac{a(h)}{V}.$$

It can be seen that dx/dz and dy/dz are functions of the flight parameters, i.e. the velocity V, the flight direction defined by the angles γ and δ, the angle Φ which determines the position of the rays in the "coupled cone" (Fig. 4), and the altitude z (W_x and W_y are components of the wind velocity, while a is the velocity of sound propagation).

If h is the flight altitude, then the time for the propagation of the N wave along any ray is

$$t = \int_0^h \frac{dl}{a(z)}dz = \int_0^h \frac{1}{a(z)}\left\{\left(\frac{dx}{dz}\right)^2 + \left(\frac{dy}{dz}\right)^2 + 1\right\}^{1/2} dz.$$

Condition (1) takes then the form

$$\left[\int_0^h \frac{1}{a(z)}\left\{\left(\frac{dx}{dz}\right)^2 + \left(\frac{dy}{dz}\right)^2 + 1\right\}^{1/2} dz\right]_{t=t_1}$$

$$= t_2 - t_1 + \left[\int_0^h \frac{1}{a(z)}\left\{\left(\frac{dx}{dz}\right)^2 + \left(\frac{dy}{dz}\right)^2 + 1\right\}^{1/2} dz\right]_{t=t_2}. \tag{3}$$

The quantities V, γ and δ, i.e. the arguments of the functions dx/dz, dy/dz and h, which describe the flight, are, in general, functions of time.

At the point (x, y), where focussing occurs, the two or more intersecting rays will, in general, have different angles Φ (Fig. 3). (In the particular case

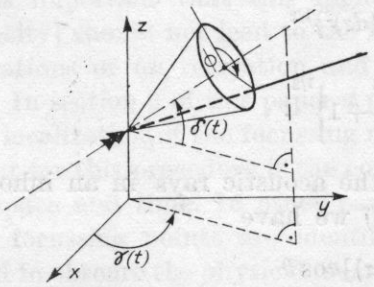

Fig. 4. Definition of the angles γ and δ describing the flight direction

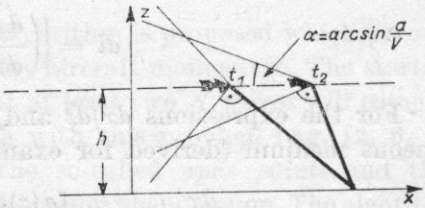

Fig. 5. Focussing of N waves beneath the flight path

of the focussing, occurring directly under the flight path, $\Phi_1 = \Phi_2$). Equation (3) is thus dependent on the angles Φ_1, Φ_2 and the times of emission t_1, t_2:

$$H_1(t_1, t_2, \Phi_1, \Phi_2) = 0. \tag{4}$$

The apparent form of this relation can only be determined when all quantities in the expressions dx/dz, dy/dz (formula (2)), and the altitude h are known functions, e.g. $V(t) = V_0 + mt$, $a(z) = a_0(1-\beta z)$, $h = h_0$ etc.

If we assume that at $t = 0$ the aircraft is at the point $x = 0$, $y = 0$, $z = h$, then by integration of differential equations (2) we obtain the coordinates of the point at which the ray emitted at a time t_i $(i = 1, 2)$ meets the earth's surface:

$$x_i = X(t_i) + \left[\int_0^h f_1(V, \gamma, \delta, \Phi, z)\,dz\right]_{t=t_i}, \tag{5}$$

$$y_i = Y(t_i) + \left[\int_0^h f_2(V, \gamma, \delta, \Phi, z)\,dz\right]_{t=t_i}. \tag{6}$$

$X(t_i)$, $Y(t_i)$, $h(t_i)$ determine the position of the aircraft at the time of emission of the i-th N wave.

Using the definition of angles γ and δ (Fig. 4), we have

$$X(t_i) = \int_0^{t_i} V\cos\gamma\cos\delta\,dt, \qquad Y(t_i) = \int_0^{t_i} V\sin\gamma\cos\delta\,dt. \tag{7}$$

If the conditions $x(t_1) = x(t_2)$ and $y(t_1) = y(t_2)$ are introduced into (5) and (6), which denote that the focussing will take place only when the two N waves emitted at the moments t_1 and t_2 will meet at the same point on the

earth's surface (Fig. 3), we obtain equations which, like the condition for the synchronization of the sonic booms (equation (4)), can be rewritten in the form

$$H_2(t_1, t_2, \Phi_1, \Phi_2) = 0, \quad H_3(t_1, t_2, \Phi_1, \Phi_2) = 0.$$

From these equations, eliminating Φ_1 and Φ_2, we obtain

$$t_2 = f(t_1). \tag{8}$$

This equality shows that at the point (x, y) there will occur a superposition of the waves emitted at times t_1 and $f(t_1)$. It is obvious that different manoeuvres (i.e. variations of the flight with time) and different atmospheric conditions, described by $a(z)$, $W_x(z)$ and $W_y(z)$, will give different forms for the function f. If the three above-mentioned equations do not take the form of equation (8), the focussing will not take place.

Let us assume that the functional relation (8) exists for the interval (t_1', t_2''). For any time t_1 within this interval, a time t_2 can be found which corresponds to the time of emission of the N wave which coincides at the same point with the wave emitted at time t_1. For these times from equations (5) and (6) we obtain a set of coordinates $\{x, y\}$ at which focussing occurs.

3. The location of the ground focus line produced by a supersonically accelerating aircraft (for the particular case of linear travel)

It has already been stated that manoeuvres involving a change of flight direction can result in the phenomenon of focussing which can be of hazard. Thus, irrespective of such considerations as comfort and safety during the flight, planned flight paths are straight lines. During such a flight only one manoeuvre is performed which may cause focussing – the initial acceleration. The uniform retardation in the last stages of the flight does not cause focussing.

The procedure, proposed here, for the localization of the focus of the sonic boom differs from the algorithm previously proposed. This procedure is based on the phenomenon which in the most simple manner can be explained on the assumptions that the medium, in which the N wave is propagating, is homogeneous (i.e. no refraction occurs), and the rays are thus straight lines.

If the aircraft is flying at a constant altitude h along the x-axis at a varying speed $V(t)$, then the condition for the synchronization (1) of the rays beneath the flight path takes the form

$$\frac{h}{a}\left[\frac{V}{\{V^2-a^2\}^{1/2}}\right]_{t=t_1} = t_2 - t_1 + \frac{h}{a}\left[\frac{V}{\{V^2-a^2\}^{1/2}}\right]_{t=t_2}. \tag{9}$$

From the condition for the intersection at the same point of two rays along which the N waves propagate at two different times, i.e. from $x(t_1) =$

$= x(t_2)$, we obtain

$$\int_{t_1}^{t_2} V(t)\,dt = \left[\frac{h_a}{\{V^2-a^2\}^{1/2}}\right]_{t=t_1} - \left[\frac{h_a}{\{V^2-a^2\}^{1/2}}\right]_{t=t_2}. \tag{10}$$

Assuming that the aircraft is flying with uniform acceleration $V = a+mt$, and at time $t = 0$, the angle aperture of the Mach cone is $\alpha = \frac{1}{2}\pi$, since

$$\lim_{t\to 0} \arcsin\frac{a}{a+mt} = \frac{1}{2}\pi.$$

The intersection of the x-axis with the N wave propagating along the rays (Fig. 6) lies at infinity. With increasing velocity this point approaches the coordinate origin and later moves away from it.

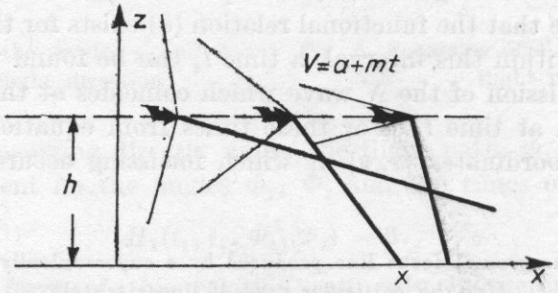

Fig. 6. The "motion" of the point of intersection of a ray with the x-axis during accelerated flight (x is the point of minimum range)

Let us denote by x the point of intersection nearest to the origin of the coordinate system and call it *the point of minimum range.*

A similar phenomenon will be observed along any straight line parallel to the x-axis (i.e. for all y), even when the rays are curved, as in the case of the earth's (refractive) atmosphere. The points of minimum range are also focussing points for the sonic boom.

If at $t = 0$ the aircraft is passing the point $x = 0$, then the point of intersection of the N wave (emitted at time t) with the x-axis has the coordinate

$$x(t) = \int_0^t (a+mt)\,dt + \frac{ha}{\{(a+mt)^2-a^2\}^{1/2}}.$$

If the acceleration is not too high and the inequality

$$\frac{mt}{a} \ll 1 \tag{11}$$

is satisfied, then from $dx(t)/dt = 0$ we obtain

$$t = \frac{h^{2/3}}{2(am)^{1/3}}, \tag{12}$$

which determines the time of emission of the N wave reaching the point of minimum range x.

Under condition (11), equations (9) and (10) take the form

$$a(t_2-t_1) = h\left(\frac{1+\frac{mt_1}{a}}{\sqrt{2\frac{mt_1}{a}}} - \frac{1+\frac{mt_2}{a}}{\sqrt{2\frac{mt_2}{a}}}\right),$$
$$a(t_2-t_1)+\frac{1}{2}m(t_2^2-t_1^2) = h\left(\frac{1}{\sqrt{2\frac{mt_1}{a}}} - \frac{1}{\sqrt{2\frac{mt_2}{a}}}\right). \tag{13}$$

The first of these equations relates to the times of emission $\{t_1, t_2\}$ of the sonic booms which reach the earth's surface at the same time, but not necessarily at the same place. The second equation relates to pairs $\{t_1, t_2\}$ which correspond to the times of emission of the N waves reaching the same point, but not necessarily at the same time. In order to find the points of focussing it is necessary to find the pairs $\{t_1, t_2\}$ which simultaneously satisfy the two equations.

If $mh/a^2 \ll 1$, then from equations (13) we obtain

$$t_2 = \frac{h}{\sqrt{2\,amt_1}} \quad \text{and} \quad t_1 = t_2 = \frac{h^{2/3}}{2(am)^{1/3}}.$$

Thus the focussing takes place at the point of minimum range, as if the ray during its travel along the x-axis stopped at this point (Fig. 8). This results in the superposition of the N waves.

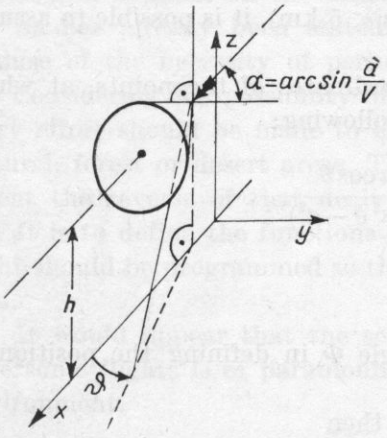

Fig. 7. The definition of the angle ϑ describing the position of a ray within the coupled cone

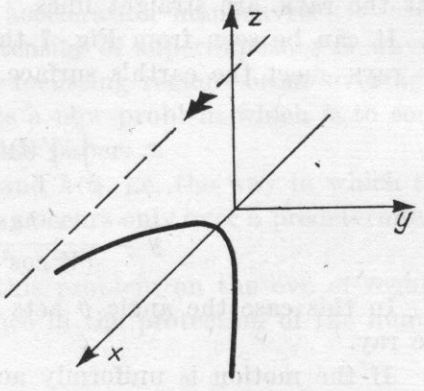

Fig. 8. The curve along which focussing occurs (equation (15))

Since the points of minimum range for accelerated rectilinear flying occur over the whole area of sonic boom audibility, and not only beneath the flight path as is shown in Fig. 6, it is obvious that the points of focussing lie on a curve which is symmetrical relative to the flight path (Fig. 8).

The identity of the points of minimum range with the points of focussing largely facilitates their determination.

During the rectilinear flight along the x-axis, $\gamma = 0$ and $\delta = 0$ (in Fig. 4). This simplifies equation (5) to the form

$$x_i = \int_0^{t_i} V(t)\,dt + \left[\int_0^h f_1(V, \Phi, z)\,dz\right]_{t=t_i},$$

$$y_i = \left[\int_0^{t_i} f_2(V, \Phi, z)\,dz\right]_{t=t_i}.$$

Eliminating the parameter Φ, we have

$$x(t_i) = \int_0^{t_i} V(t)\,dt + \left[\int_0^h f_1(V, y, z)\,dz\right]_{t=t_i}. \tag{14}$$

The times of emission of the N waves, which reach the points of minimum range, are obtained from the equation

$$\frac{dx(t_i)}{dt_i} = 0,$$

whence we may obtain the function in the form $t_i = h(y)$. Substituting this relation into equation (14) we obtain a set of focal points in the form (Fig. 8)

$$x = f(y).$$

Let us illustrate this procedure with an example. If the rectilinear flying is effected at a comparatively small altitude ($h < 5$ km), it is possible to assume that the rays are straight lines.

It can be seen from Fig. 7 that the coordinates of the points, at which the rays meet the earth's surface, are the following:

$$x = \int_0^t V(t)\,dt + \frac{ha\cos\vartheta}{(V^2\cos^2\vartheta - a^2)^{1/2}},$$

$$y = \frac{ha\sin\vartheta}{(V^2\cos^2\vartheta - a^2)^{1/2}}.$$

In this case the angle ϑ acts as the angle Φ in defining the position of the ray.

If the motion is uniformly accelerated, then

$$\int_0^t V(t)\,dt = \frac{V^2 - a^2}{2m}.$$

In this case it is preferable to use the velocity V rather than the time t. We may further obtain

$$x(t) = \frac{V^2 - a^2}{2m} + \frac{a\sqrt{h^2 + y^2}}{(V^2 - a^2)^{1/2}},$$

corresponding to equation (14).

Differentiating $x(t)$ with respect to t we obtain

$$1 - a\{h^2 + y^2\}^{1/2}\{V^2 - a^2\}^{-3/2} m = 0.$$

The value V, which satisfies this equation, corresponds to the time of emission of the N wave of the shortest range. Eliminating V from the last two equations, we obtain the equations of the loci along which the focussing occurs:

$$y^2 - \frac{8}{27}\frac{m}{a^2} x^3 + h^2 = 0. \tag{15}$$

WANNER [7] has obtained the same result by another method.

4. Conclusions

Due to changing flight parameters (a manoeuvre), the phenomenon of focussing may occur during flights at supersonic speeds.

On the basis of the algorithms, proposed in sections 2 and 3, the location of the focus may be determined if data describing the flight are known. Relevant data are the velocity $V(t)$, the angles γ and δ that characterize the direction, the altitude $h(t)$ and the velocity of sound propagation in the atmosphere $a(z)$ (which depends on the altitude).

As has already been stated, the focussing phenomenon is unavoidable because of the necessity of performing an acceleration manoeuvre.

Considering the possibility of a high intensity of superimposing N waves, every effort should be made to ensure that focussing regions occur over agricultural, forest or desert areas. This presents a new problem which is to some extent the reverse of that dealt with in this paper.

It is to define the functions $V(t)$, $\delta(t)$ and $h(t)$, i.e. the way in which the flight should be programmed so that focussing occurs only over a predetermined area.

It would appear that the solution of this problem on the eve of regular supersonic flights is of paramount importance in the protection of the human environment.

Acknowledgment. The author is greatly indebted to Professor H. RYFFERT, chief of the Chair of Acoustics at A. Mickiewicz University, Poznań, for discussion and helpful remarks.

References

[1] R. MAKAREWICZ, *Equations of acoustic rays in an inhomogeneous moving medium*, Archives of Acoustics, **1**, 1, 21–28 (1976).

[2] J. NICHOLLS, B. JAMES, *The location of the ground focus line produced by a transonically accelerating aircraft*, J. Sound and Vibration, **20**, 145–168 (1972).

[3] R. ONYEONWU, *Sonic boom signatures and ray focussing*, J. Sound and Vibration, **42**, 85–101 (1975).

[4] H. RIBNER, *Supersonic turns without superbooms*, J. Acoust. Soc. Amer., 52, 1037–41 (1972).

[5] A. TARNOGRODZKI, E. ŁUCZYWEK, *Approximate method of determination of the location of a sonic boom in the accelerated motion of an aircraft*, Arch. Mech. Stos., **19**, (1967).

[6] J. WANNER, *Theoretical and experimental studies of the focus of sonic booms*, J. Acoust. Soc. Amer., **52**, 13–32 (1972).

[7] C. H. E. WARREN, *The propagation of sonic bangs in a nonhomogeneous still atmosphere*, 4th Congress Aeronautical Sciences, London 1964.

Received on 12th July 1976

ARCHIVES OF ACOUSTICS
2, 3, 177-188 (1977)

MEASUREMENT OF THE VISCOELASTIC CONSTANTS OF THE CELLULOSE USED FOR A LOUDSPEAKER MEMBRANE AND THEIR EFFECT UPON THE ELECTRO-ACOUSTIC PARAMETERS OF THE LOUDSPEAKER

ANDRZEJ DOBRUCKI, CZESŁAW ADAM ROSZKOWSKI

Institute of Telecommunication and Acoustics of Wrocław Technical University (Wrocław)

The concept of a complex Young's modulus, characterizing the properties of materials with internal loss, has been introduced. The methodology of the measurement of Young's modulus and a detailed description of the method of measuring this quantity for cellulose used for a loudspeaker membrane is given. Results of measurements of the viscoelastic parameters of six kinds of cellulose are presented, and a marked influence of the absolute value of the complex Young's modulus for cellulose on the upper frequency limit of a loudspeaker with a membrane made of this cellulose is shown. Subjective investigations of loudspeakers have confirmed this conclusion.

1. Introduction

In previous works on the theory and design of loudspeakers it has been assumed that Young's modulus of the membrane material is a constant and real. No consideration has been given to the losses involved and it has also been assumed that the modulus has a constant value which is independent of frequency.

The purpose of this paper is to show the dependence of the complex Young's modulus and loss factor on the frequency. Thereafter, a method is presented for the measurement of the mechanical properties of materials used for the production of loudspeaker membranes and the results of measurements of the absolute value of the complex Young's modulus and loss factor (loss angle) and their dependence on the frequency of vibration for six different kinds of cellulose. Finally, the results of an experiment are presented which was aimed at determining the effect of the material of which the loudspeaker membrane is made on its acoustic properties. The experiment involved the construction of 18 loudspeakers of the same type, differing only in the kind of cellulose from which their membranes were made (from each kind of cellulose, three loudspeakers were made).

2. The Young's complex modulus

For linear elastic bodies we have the relation called *Hooke's law*. This relation in a Cartesian system of coordinates, using the notation of tensor calculus, takes the form

$$\sigma_{ij} = C_{ijkl} e_{kl}, \tag{1}$$

where σ_{ij} represents the stress tensor, e_{kl} – the strain tensor, and C_{ijkl} – the tensor of elasticity constants.

In the case of an isotropic material the number of independent components of the tensor of elasticity constants is reduced to two. Equation (1) can then take the form

$$\sigma_{kk} = G_2 e_{kk}, \qquad \sigma'_{ij} = G_1 e'_{ij}, \tag{2}$$

where G_1 denotes the shear modulus, G_2 – the modulus of all-sided (all-round) compression, e'_{ij} – the strain deviator, and σ'_{ij} – the stress deviator.

The deviators of strain and stress are given by equations (2a) and (2b) respectively:

$$e'_{ij} = e_{ij} - \frac{1}{3} e_{kk} \delta_{ij}, \tag{2a}$$

$$\sigma'_{ij} = \sigma_{ij} - \frac{1}{3} \sigma_{kk} \delta_{ij}. \tag{2b}$$

It is possible to present equation (1) as follows:

$$e_{ij} = \frac{1+\nu}{E} \sigma_{ij} - \frac{\nu}{E} \sigma_{kk} \delta_{ij}. \tag{3}$$

Between the constants G_1 and G_2, Young's modulus E and Poisson's ratio ν there are the explicit relations (4):

$$E = \frac{3G_1 G_2}{2G_2 + G_1}, \qquad \nu = \frac{G_2 - G_1}{2G_2 + G_1}. \tag{4}$$

For lossy materials these relations become more complicated, and the interdependence of the stress and the strain at a given moment depends on the whole of the preceding relations between these two magnitudes. Hooke's law for materials of this type can be expressed using an integral convolution

$$\sigma_{ij}(t) = \int_{-\infty}^{t} G_{ijkl}(t-\tau) \frac{\partial e_{kl}(\tau)}{\partial \tau} d\tau, \tag{5}$$

where $G_{ijkl}(t-\tau)$ is the tensor relaxation function. Equation (2) can be written in the form

$$\sigma_{kk}(t) = \int_{-\infty}^{t} G_2(t-\tau)\frac{\partial e_{kk}(\tau)}{\partial \tau}\,d\tau,$$
$$\sigma'_{ij}(t) = \int_{-\infty}^{t} G_1(t-\tau)\frac{\partial e'_{ij}(\tau)}{\partial \tau}\,d\tau. \tag{6}$$

It is assumed that the strain $e_{ij}(\tau)$, and thus also the strains $e'_{ij}(\tau)$ and $e_{kk}(\tau)$ are sinusoidal functions of time,

$$e_{kk}(\tau) = \bar{e}_{kk}e^{j\omega\tau}, \qquad e'_{ij}(\tau) = \bar{e}'_{ij}e^{j\omega\tau}, \tag{7}$$

where $\bar{e}'_{ij}$ and $\bar{e}_{kk}$ are independent of time. It is also assumed that the motion lasts infinitely long, thus nonstationary states can be neglected. Substituting $\xi = t-\tau$, we obtain

$$\sigma_{kk}(t) = j\omega e_{kk}e^{j\omega t}\int_{-\infty}^{+\infty} G_2(\xi)e^{-j\omega\xi}\,d\xi,$$
$$\sigma'_{ij}(t) = j\omega e'_{ij}e^{j\omega t}\int_{-\infty}^{+\infty} G_1(\xi)e^{-j\omega\xi}\,d\xi. \tag{8}$$

The integrals in formula (8) are Fourier transformations of the relaxation functions $G_2(t)$ and $G_1(t)$. These transformations, when multiplied by $j\omega$, are written respectively as

$$j\omega\int_{-\infty}^{+\infty} G_2(\xi)e^{-j\omega\xi}\,d\xi = \bar{G}_2(j\omega),$$
$$j\omega\int_{-\infty}^{+\infty} G_1(\xi)e^{-j\omega\xi}\,d\xi = \bar{G}_1(j\omega). \tag{9}$$

The quantities $\bar{G}_2(j\omega)$ and $\bar{G}_1(j\omega)$ are called respectively the *complex compression modulus* and *complex shear modulus*.

While for elastic materials the elasticity constants E and ν are used, for viscoelastic materials one can introduce a complex Young's modulus $\bar{E}(j\omega)$ and a complex Poisson's ratio $\bar{\nu}(j\omega)$:

$$\bar{E}(j\omega) = \frac{3\bar{G}_1(j\omega)\bar{G}_2(j\omega)}{2\bar{G}_2(j\omega)+\bar{G}_1(j\omega)},$$
$$\bar{\nu}(j\omega) = \frac{\bar{G}_2(j\omega)-\bar{G}_1(j\omega)}{2\bar{G}_2(j\omega)+\bar{G}_1(j\omega)}. \tag{10}$$

Poisson's ratio over a frequency range of about 20 kHz [1] is real and independent of the frequency. The phase angle δ of Young's modulus is called *loss angle* while the tangent of this angle is termed the *loss factor*.

3. Measurement of the complex Young's modulus

The method of measuring the complex Young's modulus is based on the measurement of resonance frequencies and of widths of the resonance bands of a bar of the material to be tested. This bar is free at one end, clamped at the other and induced to vibrate transversely [4]. The measurement system is shown in Fig. 1. A specimen of the material is placed in the exciter which

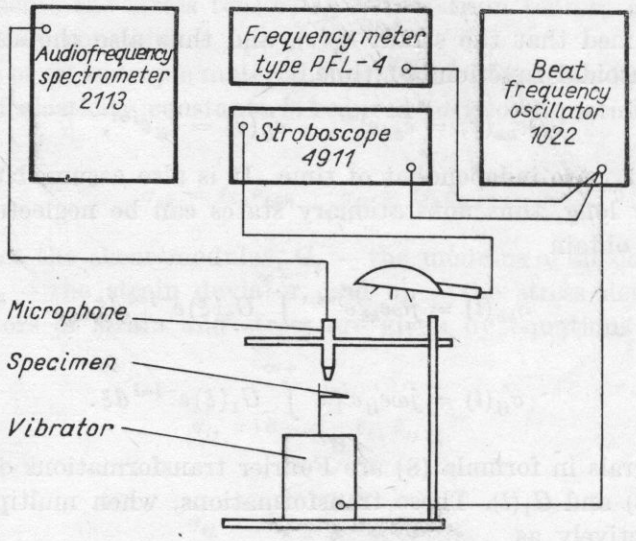

Fig. 1. System for measuring the complex Young's modulus

is driven by a generator of sinusoidal vibrations. The vibrating bar produces in its proximity an acoustic pressure proportional to the amplitude of vibrations. This pressure is measured using a microphone and a spectrometer. With the aid of a stroboscope one seeks, while tuning the generator by hand, successive modes of vibration. The frequencies of these modes are read by means of a precise frequency meter. By detuning the generator one obtains, in the proximity of a given mode of vibration, two frequencies for which the pressure level drops by 3 dB below the pressure level at resonance. These frequencies determine the band width of a given resonance. The complex Young's modulus is evaluated from the formula

$$\underline{E} = (1+jd)\cdot 4.8\pi^2\varrho\left(\frac{l^2}{h^2}\frac{f_n}{k_n}\right)^2, \tag{11}$$

where ϱ denotes the density of the material [kg/m^3], l – the active length of the bar [m], h – the thickness of the bar [m], f_n – the frequencies of successive modes of vibration [Hz], and d – the loss factor.

The values of the coefficients k_n depend only on the number n of the mode of vibration and are stated in Table 1.

Table 1. Values of the coefficient k_n for the first eight modes of vibration

Mode No.	1	2	3	4	5	6	7	8
k_n	3.52	22.0	61.7	121	200	299	417	555

4. Measurement of the Young's complex modulus of cellulose used for loudspeaker membranes

Measurements of the complex Young's modulus were made on prepared specimens of six grades of cellulose used for the production of loudspeaker membranes. The specimens were cut in the form of cellulose discs in the manner shown in Fig. 2. For each kind of cellulose about 60 specimens were cut out.

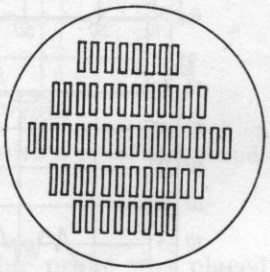

Fig. 2. The method of cutting out specimens for measurement from a pressed cellulose disc

Of these 60 specimens 10 were selected, the density and thickness of which corresponded with the prescribed tolerances to the density and thickness of loudspeaker membranes GDN 16/10.

All the specimens were cut out by means of one punch die. The shape and dimensions of the specimens are presented in Fig. 3. The specimen was

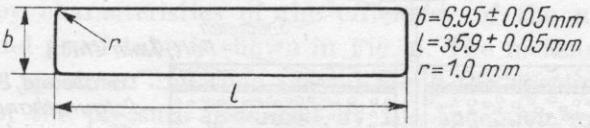

Fig. 3. Measurement specimen

then placed in the vibrator. For the measurements the vibrator produced by WZG TONSIL was used. It is constructed on the basis of a high-power loudspeaker.

In an anechoic chamber the pressure to frequency characteristics of the sound radiated by the exciter was measured. During this measurement the

microphone was located at the same place as it was during measurements of the specimens. In order to ensure a correct measurement, the level of the sound emitted by the vibrator should be smaller by at least 20 dB than the level of the pressure produced by the specimen at the location of the measuring microphone. Since the vibrator did not satisfy this condition, sound emitted by the vibrator was attenuated. The method of attenuation is shown in Fig. 5. The frequency characteristics of the sound emitted by the vibrator before and after attenuation is presented in Fig. 4.

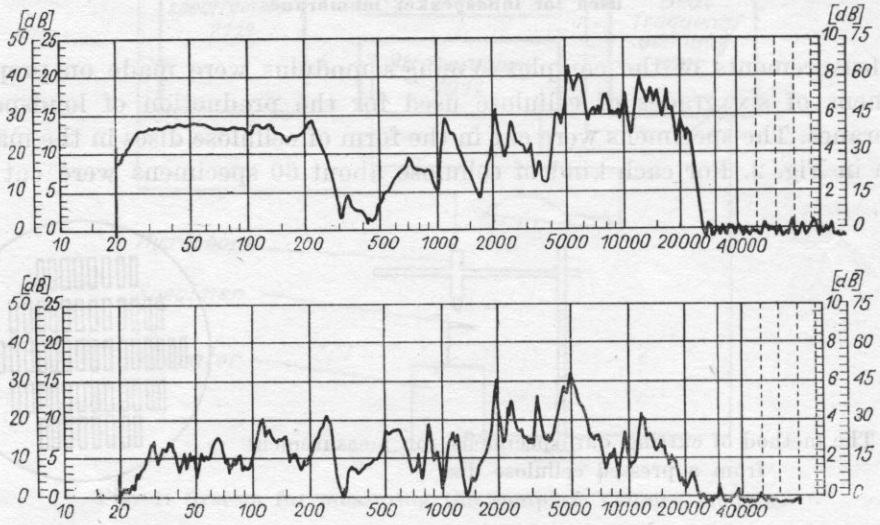

Fig. 4. Frequency characteristics of the sound emitted by the exciter before and after attenuation

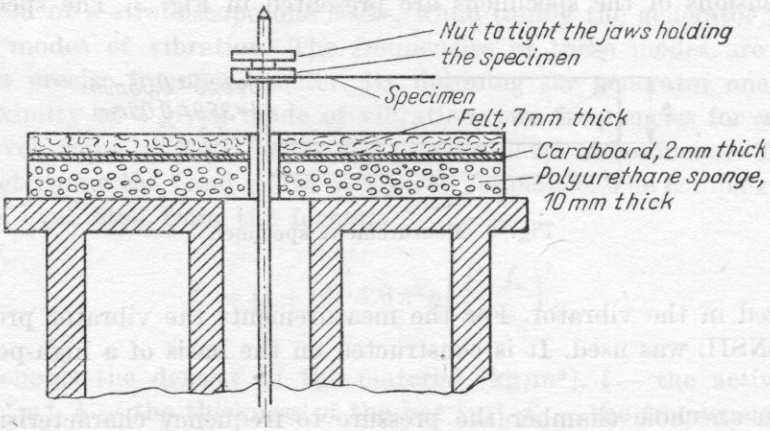

Fig. 5. The method of attenuating the exciter and of mounting the specimen in the exciter

The specimens were placed in the jaws of the vibrator with a constant pressure. Due to the lack of a torgue wrench this was done by tightening the nut so that a mark on the nut was always in the same position. The precision of the constant pressure was thus of the same order as the precision in selecting the specimen thickness. Nevertheless, the inaccuracy in establishing the pressure force was chiefly the main reason for measurement errors. In future measurements with torgue wrenches it will be absolutely necessary to obtain a certain constant pressure force. The procedure of mounting the specimen in the vibrator is shown in Fig. 5.

Measurement of the pressure level produced by the specimen was performed with a 1/2 in. microphone B&K type 4134. Since the front of the microphone

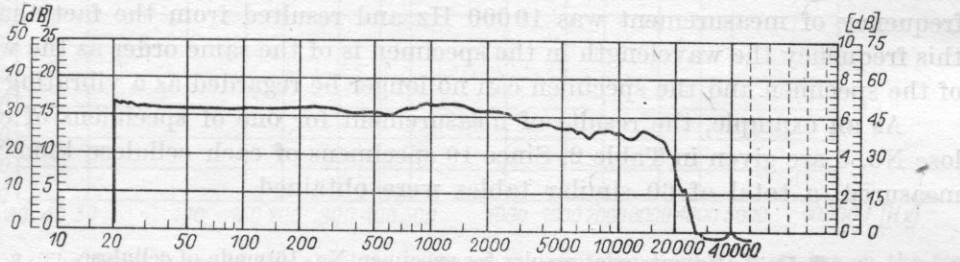

Fig. 6. Frequency characteristics of the efficiency of a microphone with a probe and sound-proof tube

was overlarge in relation to the specimen width, a tubular probe was placed on the microphone. This greatly facilitated the handling of the microphone over the specimen during the measurements, reduced disturbances due to the microphone and meant that the microphone did not integrate the pressure over the whole of the specimen area but received the pressure approximately from one point. Since the resonance of a microphone with such probe occurs at a frequency of about 5500 Hz, the tube was made sound-proof with fibrous material.

The frequency characteristics of the efficiency of the microphone with its probe and sound-proof tube is shown in Fig. 6. The measuring microphone is placed over the specimen and then moved along the specimen to the place where the level of the pressure produced by the specimen was highest. E.g. for the second mode of vibration, the position of the microphone over the specimen is shown in Fig. 7.

Since the resonance frequencies of free vibration of the bar are distributed rather rarely, the specimen was shortened during the measurement process. The length of the shortened specimen was measured with an accuracy of 0.1 mm, and the measurements were repeated. In this manner new resonance frequencies ranging between the resonance frequencies of the specimen before its shortening were obtained. When the number of measuring points was still

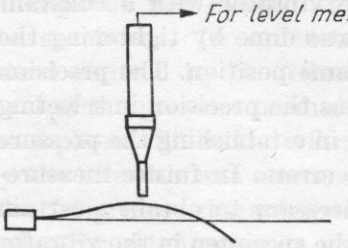

Fig. 7. An example of placing the microphone over the specimen at modes of vibration other than the fundamental

too small, the specimen was again shortened. The specimen not be shortened to more than half of its original length because it then stops vibrating as a bar and begins to behave as a plate, thus introducing large errors. The upper frequency of measurement was 10000 Hz and resulted from the fact that at this frequency the wavelength in the specimen is of the same order as the width of the specimen and the specimen can no longer be regarded as a vibrating bar.

As an example, the results of measurement for one of specimens of cellulose No. 6 are given in Table 2. Since 10 specimens of each cellulose kind were measured, a total of 60 similar tables were obtained.

Table 2. Measurement results for specimen No. 16 made of cellulose No. 6

ϱ [kg/m^3]	h [m]	f_n [Hz]	Δf_n [Hz]	d	l [m]	Mode No.
		95.1	8.0	0.08412	0.03375	1
		161.7	13.0	0.08040	0.02575	1
		284.0	20.1	0.07074	0.02000	1
		420.1	27.9	0.06641	0.01765	1
		652.0	35.0	0.05368	0.03375	2
		1071.0	47.5	0.04435	0.02575	2
454	0.000426	1847.0	66.5	0.03600	0.02000	2
		1851	61	0.03300	0.03375	3
		2960	133	0.04493	0.02575	3
		3479	130	0.03737	0.03375	4
		5965	262	0.04392	0.03375	5
		8521	330	0.03873	0.03375	6

The values of the loss factor have been calculated directly from the resonance curves, while the absolute values of the complex Young's modulus have been calculated from formula (11). As an example, the results of measurements in the form of graphs for cellulose No. 6 are shown together with measuring points in Figs. 8 and 9. It can be seen from these figures that the scatter of the measurements is considerable. For this reason the measured points for all cellulose kinds are not given in this paper. Only averaged mean curves of

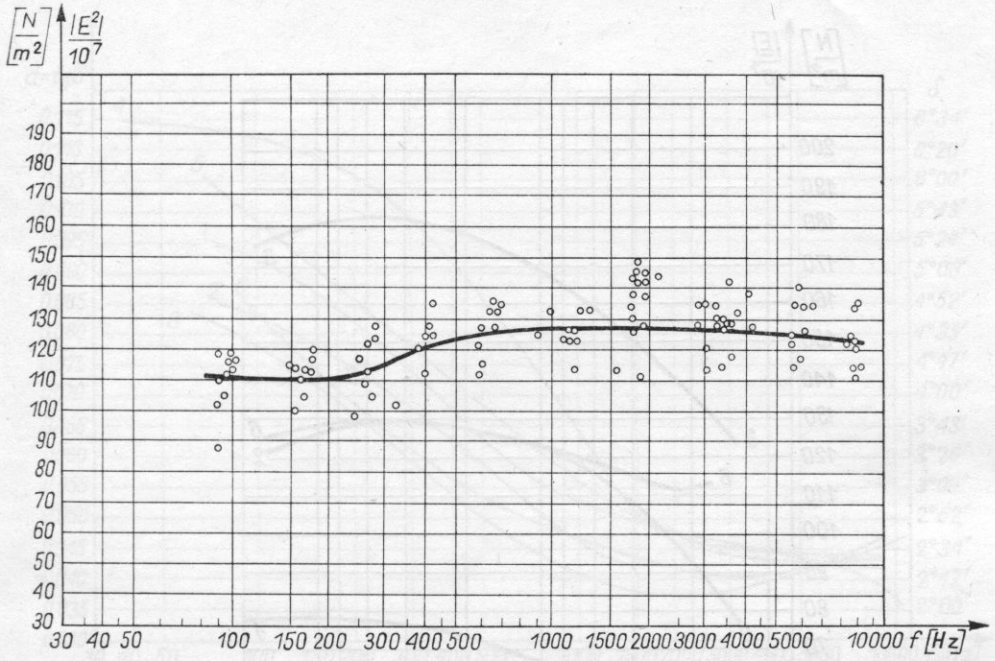

Fig. 8. The dependence of the absolute value of the complex Young's modulus on the frequency of vibration for cellulose No. 6

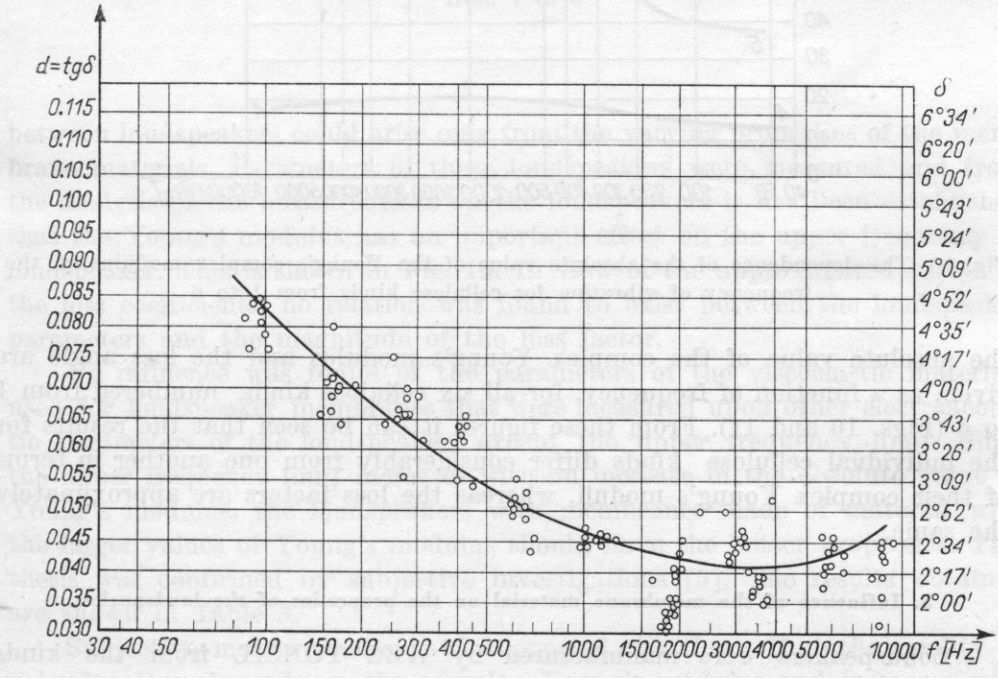

Fig. 9. The dependence of the value of the loss factor on the frequency of vibration for cellulose No. 6

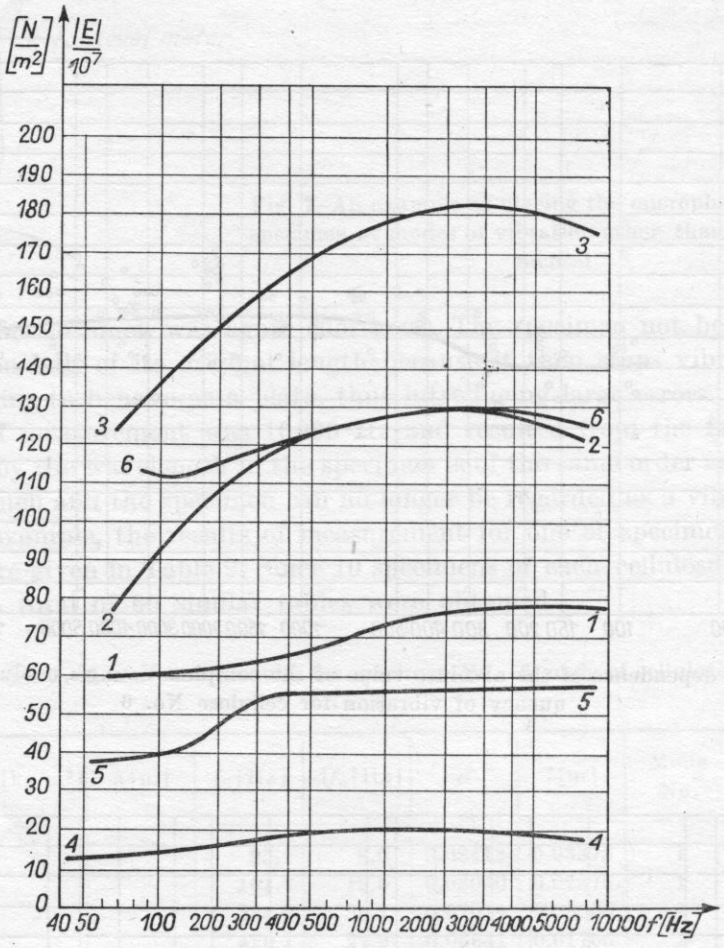

Fig. 10. The dependence of the absolute value of the Young's complex modulus on the frequency of vibration for cellulose kinds from 1 to 6

the absolute value of the complex Young's modulus and the loss angle are given, as a function of frequency, for all six cellulose kinds numbered from 1 to 6 (Figs. 10 and 11). From these figures it can be seen that the results for the individual cellulose kinds differ considerably from one another in terms of their complex Young's moduli, whereas the loss factors are approximately the same.

5. Influence of the membrane material on the properties of the loudspeaker

Loudspeakers were manufactured by WZG TONSIL from the kinds of cellulose tested, according to loudspeaker specifications GDN 16/10. All the design requirements of loudspeakers were strictly met, so that differences

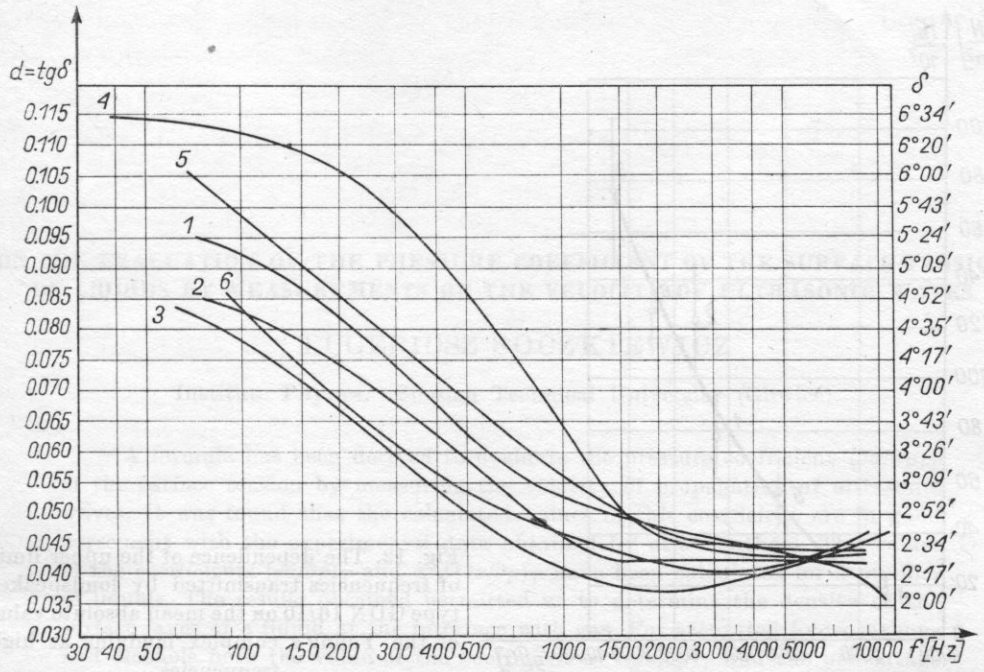

Fig. 11. The dependence of the loss factor on the frequency of vibration for cellulose kinds from 1 to 6

between loudspeakers could arise only from the varying properties of the membrane materials. Parameters of these loudspeakers were measured and from the analysis of the measurements on the loudspeakers it has been established that the Young's modulus has an important effect on the upper frequency of loudspeaker. This is shown in Fig. 12. In view of the approximated values of the loss coefficients, no relation was found to exist between the loudspeaker parameters and the magnitude of the loss factor.

No influence was found of the parameters of the viscoelastic materials used for loudspeaker membranes that were measured upon other electroacoustic parameters of the loudspeaker, except the upper frequency limit. Since the upper frequency limit increases with an increase in the absolute value of Young's modulus, the loudspeakers with membranes made of material with the larger values of Young's modulus should have the better properties. This thesis was confirmed by subjective investigations [5]. The results obtained are shown in Table 3.

Subjective measurements have supported the thesis that the quality of a loudspeaker depends on the complex Young's modulus and increases with an increase in the absolute value of the latter.

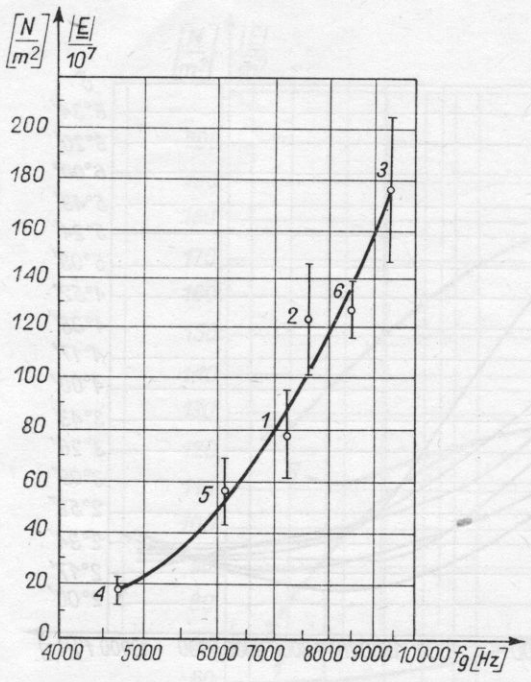

Fig. 12. The dependence of the upper limit of frequencies transmitted by loudspeaker type GDN 16/10 on the mean absolute value of the Young's complex modulus at high frequencies

Table 3. Results of the acoustic investigation of loudspeakers with membranes made from the cellulose kinds tested

Loudspeaker with membrane of cellulose No.	1	2	3	4	5	6
Fraction of voice in subjective measurements	0.51	0.63	0.70	0.13	0.40	0.62

References

[1] D. R. Bland, *The theory of linear viscoelasticity*, Pergamon Press, Oxford, London, New York, Paris 1960.

[2] D. R. Bland, E. H. Lee, *Calculation of complex modulus of linear viscoelastic materials from vibrating reed measurements*, Journal of Applied Physics, **26**, 12, 1497–1503 (1955).

[3] A. Dobrucki, Cz. A. Roszkowski, *Measurement of the Young's complex modulus of cellulose used for loudspeaker membranes*, Proceedings of 23rd Open Seminar on Acoustics, Wisła 1976, p. 179.

[4] Cz. A. Roszkowski, *The influence of the material used for loudspeaker membrane upon the acoustic properties of the loudspeaker*. Dissertation. Institute of Telecommunication and Acoustics, Wrocław 1976, p. 16.

[5] Z. Żyszkowski, A. Dobrucki, C. Szmal, *Studies on the relation between the synthetic index of quality and acoustic (auditory) measurements*. Report No. 128/R-060/76, Institute of Telecommunication and Acoustics, Wrocław Technical University, Wrocław 1976, p. 52.

Received on 8th December 1976

ARCHIVES OF ACOUSTICS
2, 3, 189-196 (1977)

ON THE EVALUATION OF THE PRESSURE COEFFICIENT OF THE SURFACE TENSION OF LIQUIDS BY MEASUREMENTS OF THE VELOCITY OF ULTRASONIC WAVES

EUGENIUSZ SOCZKIEWICZ

Institute Physics, Silesian Technical University (Gliwice)

A formula has been derived to evaluate the pressure coefficient $(\partial\sigma/\partial p)_T$ of the surface tension by measuring the velocity of propagation of ultrasonic waves. It was found that the calculated values of this coefficient are in good agreement with the experimental data obtained by other authors. The values of the coefficients $(\partial\sigma/\partial p)_T$ and $\sigma^{-1}(\partial\sigma/\partial p)_T$ have been calculated for a number of liquids. The results obtained permitted us to determine the density of the surface layer of a liquid at the interface with gas. For saturated hydrocarbons and alcohols both the value of the coefficient $\sigma^{-1}(\partial\sigma/\partial p)_T$ and the percentage reduction of the density, of the surface layer in relation to the liquid density decrease monotonically with the increasing length of the chains of molecules in a given chemical compound.

1. Introduction

The effect of pressure on the value of the surface tension of liquids depends on the kind of gas above the liquid surface. The solution of gas in the liquid leads to a reduction on its surface tension [3, 8-10]. RUSANOV [8], and also SAHLI [9] have found experimentally that the surface tension of liquids increases with increasing pressure, only when the gas above the liquid neither dissolves in it, nor is subject to absorption by the surface layer. In the papers cited the gas used to obtain the pressure [8] was helium or the pressure was produced by means of centrifugal forces [9] to avoid the solution of gas in the boundary layer. Further consideration concerns the effect of pressure on the surface tension of liquids, when the gas does not dissolve in the boundary layer.

2. Empirical relationships defining the pressure dependence of the surface tension of liquids

PARTINGTON, in his monograph [6], gives a number of empirical relations between the isothermal compressibility of a liquid and its surface tension. Thus, according to RICHARDS and PALITZSCH, the relation

$$\beta_T^{\dagger}\sigma^{4/3} = 2.53 \times 10^{-3}\left[\frac{\text{dynes}}{\text{cm} \times \text{atm}}\right] \tag{1}$$

holds true over a pressure range from 100 to 500 atm, where β_T is the isothermal compressibility of the liquid and σ is the surface tension of the liquid.

According to TYRER, the relation

$$\beta_T \sigma^{4/3} = 1.2 \times 10^{-3} T^{1/3} \left[\frac{\text{dynes}}{\text{cm} \times \text{atm} \times \text{deg}^{1/3}} \right] \tag{2}$$

is satisfied for pressures up to 1 atm, where T is absolute temperature. GOPALA RAO [2], using phenomenological considerations, has established the formula

$$\sigma = \left(\frac{A}{\beta_T} \right)^{1/\tau}, \tag{3}$$

in which A and τ are constants for a given liquid.

The above formulae indicate an increase in the surface tension of liquids with increasing pressure, since the isothermal compressibility decreases with increasing pressure.

3. Eötvös' rule and the dependence of the surface tension on the pressure

It will be shown that the formula describing the pressure coefficient of the surface tension can be derived using EÖTVÖS' rule [6]

$$\sigma V^{2/3} = K(T_c - T), \tag{4}$$

where V denotes the molar volume of the liquid, T_c is the critical temperature (in Kelvin degrees), K is a coefficient independent of the temperature, and the other symbols are as stated.

At the same time it should be proved that the coefficient K is independent of pressure variations. This can be done using BRILLOUIN'S [1] generalized analysis of the various types of packing structure of molecules in liquids. According to BRILLOUIN, thermal motions of the surface molecules propagate throughout the surface in the form of capillary waves, whose phase velocity w_1, as can be easily proved are given by [4]

$$w_1 = \left(\frac{\sigma \omega}{\varrho_1} \right)^{1/3}, \tag{5}$$

where ϱ_1 is the surface density of the liquid layer and ω is the cyclic frequency of the molecular vibrations. From formula (5) we obtain

$$\omega^2 = \frac{\sigma \gamma^3}{\varrho_1}, \tag{6}$$

where γ is the wave number. For the group velocity w_2 of the capillary waves we have

$$w_2 = \frac{d\omega}{d\gamma} = \frac{3}{2} w_1. \tag{7}$$

BRILLOUIN has shown that the capillary waves apply, per unit length of the boundary of the surface, a force F which can be expressed by

$$F = \frac{w_2}{w_1}\frac{\varepsilon}{2}, \tag{8}$$

provided that the waves are completely diffused. The quantity ε in equation (8) denotes the energy of the thermal motions of molecules per unit surface area of the liquid. This energy can be expressed by

$$\varepsilon = \frac{3RT}{S_m}, \tag{9}$$

where R is the gas constant and S_m is the surface area of a monomolecular layer of a mole of the liquid. If the surface tension at an absolute temperature $T = 0$ K is denoted by σ_0, then it follows from formulae (7)-(9) that at a temperature T we have

$$\sigma = \sigma_0 - \frac{3}{4}\varepsilon = \sigma_0 - \frac{9RT}{4S_m} \tag{10}$$

which implies that

$$-\left(\frac{\partial\sigma}{\partial T}\right)_p S_m = \frac{9}{4}R, \tag{11}$$

where the area S_m of the surface can be expressed in terms of the molar volume of the liquid. This, however, requires the knowledge of the packing structure of the molecules. It can be easily shown that for a cubic packing structure with an intermolecular distance d we have the following relations (where N is Avogadro's number) for the molar volume:

$$V = Nd^3 \tag{12a}$$

in the case of a simple cubic (S.C.) structure;

$$V = \frac{4}{3\sqrt{3}}Nd^3 \tag{12b}$$

for a body centred cubic packing structure (B.C.C.);

$$V = \frac{1}{\sqrt{2}}Nd^3 \tag{12c}$$

for a face centered cubic structure (F.C.C.).

According to BRILLOUIN the surface S_m can be expressed by the formula

$$S_m = Nd^2. \tag{13}$$

From formulae (12a)-(12c) and (13) we obtain in succession:

$$S_m = N^{1/3} V^{2/3} \tag{14a}$$

for S.C. molecular packing;

$$S_m = \left(\frac{3\sqrt{3}}{4}\right)^{2/3} N^{1/3} V^{2/3} \tag{14b}$$

for B.C.C. packing;

$$S_m = 2^{1/3} N^{1/3} V^{2/3} \tag{14c}$$

for the structure with the most dense packing (F.C.C.).

From formulae (11) and (14a)-(14c) Eötvös' coefficient K for the different packing structures can be easily evaluated. We obtain the following values: 2.21×10^{-7} [JK^{-1}] for S.C. structures, 1.86×10^{-7} [JK^{-1}] for B.C.C. structures, and 1.757×10^{-7} [JK^{-1}] for F.C.C. structures.

Experimental values of the coefficient for normal liquids with spherically-symmetrical molecules are typically about 2.2×10^{-7} [JK^{-1}], and this leads to the conclusion that the packing structure of these liquids is of the S.C. type.

It can thus be concluded that Eötvös' coefficient does not change with pressure variation, provided that the packing structure of the molecules does not change at the same time, i.e. provided that the pressure is not too large. A precise statement of the limiting pressure below which the value of Eötvös' poefficient remains constant would require knowledge of the temperature cependence of the surface tension of the liquids for various pressures. These data are not available from the literature. The limit can, however, be evaluated as is shown in section 5 of this paper, to within about 10^6 [Nm^{-2}].

Since Eötvös' coefficient does not depend on the pressure, from equation (4), for pressures that are not too large, we obtain

$$\frac{1}{\sigma}\left(\frac{\partial \sigma}{\partial p}\right)_T + \frac{2}{3}\frac{1}{V}\left(\frac{\partial V}{\partial p}\right)_T = 0. \tag{15}$$

Use now the formula for the propagation velocity of ultrasonic waves,

$$w^2 = \frac{\varkappa}{\varrho \beta_T}, \tag{16}$$

where $\varkappa$ denotes the ratio of the specific heats of the liquid at constant pressure and constant volume, β_T is the isothermal compressibility of the liquid, ϱ — the density, and w — the phase velocity of the ultrasonic waves. From (15) and (16) we obtain the following expression for the pressure coefficient of the surface tension of a liquid:

$$\left(\frac{\partial \sigma}{\partial p}\right)_T = \frac{2}{3}\frac{\sigma \varkappa}{\varrho w^2}. \tag{17}$$

The values of the coefficients $(\partial\sigma/\partial p)_T$ and $\sigma^{-1}(\partial\sigma/\partial p)_T$, evaluated from formula (17) for a number of liquids, are shown in Table 1. Experimental data concerning ϱ were taken from tables by LANDOLT-BÖRNSTEIN [5], the values of the surface tension from [7], and the values of $\varkappa$ from [11]. The error of

Table 1. Values of the pressure coefficients of the surface tension of liquids $(\partial\sigma/\partial p)_T$ and $\sigma^{-1}(\partial\sigma/\partial p)_T$ obtained from formula (17) at temperature of 293 K

Substance	$(\partial\sigma/\partial p)_T \times 10^{11}$[m]	$\sigma^{-1}(\partial\sigma/\partial p)_T \times 10^{-9}$[m^{-2}N^{-1}]
bromoform	1.17	0.37
chloroform	1.82	0.67
carbon tetrachloride	1.85	0.69
carbon disulphide	2.00	0.62
bromoethane	1.64	0.68
iodoethane	1.85	0.63
n-pentane	2.33	1.40
isopentane	2.08	1.39
n-hexane	2.04	1.11
cyklohexane	1.76	0.69
n-heptane	1.93	0.95
n-octane	1.81	0.83
isooctane	1.82	0.97
n-nonane	1.67	0.73
n-decane	1.70	0.71
n-dodecane	1.61	0.63
n-tetradecane	1.57	0.59
n-hexadecane	1.55	0.56
o-xylene	1.59	0.53
m-xylene	1.62	0.56
p-xylene	1.62	0.57
toluene	1.71	0.60
benzene	1.82	0.63
nitrobenzene	1.36	0.31
methyl alcohol	1.83	0.81
ethyl alcohol	1.77	0.75
n-propyl alcohol	1.55	0.65
isopropyl alcohol	1.56	0.72
n-butyl alcohol	1.45	0.59
isobutyl alcohol	1.50	0.66

the calculated values of the pressure coefficient of the surface tension $(\partial\sigma/\partial p)_T$ does not exceed 0.3%. SAHLI [9] has experimentally obtained a value of $(\partial\sigma/\partial p)_T = 1.8 \times 10^{-11}$ [m] for alkanes and this coincides within experimental error with the mean value of the coefficient $(\partial\sigma/\partial p)_T$ calculated for these compounds in Table 1.

Furthermore, the pressure coefficients of the surface tension $\sigma^{-1}(\partial\sigma/\partial p)_T$ of a number of homological saturated hydrocarbons decrease with the increasing number of the homologue, i.e. with an increase in the length of the chain forming the molecule. A similar pattern is also observed for *n*-alcohols.

4. Computation of the density of the surface layer of a liquid from the dependence of the surface tension on pressure

RUSANOV, KOTCHUROVA and KHABAROV [8] state a relation between the pressure coefficient of the surface tension of a liquid and the relative change of density of the surface layer of the liquid,

$$\frac{\varrho - \varrho_1}{\varrho} = \frac{1}{\delta}\left(\frac{\partial\sigma}{\partial p}\right)_T, \tag{18}$$

Table 2. Density ϱ_1 of the surface layer of various liquids at 293 K, evaluated from formula (19)

Substance	$\left(\frac{V}{N}\right)^{1/3} \times 10^{10}$ [m]	ϱ [kg m^{-3}]	ϱ_1 [kg m^{-3}]	$\frac{\varrho - \varrho_1}{\varrho} 100\,\%$
bromoform	5.26	2890	2826	2.23
chloroform	5.11	1487	1434	3.56
carbon tetrachloride	5.43	1594	1540	3.40
carbon disulphide	4.64	1264	1209	4.32
bromoethane	4.98	1461	1413	3.29
iodoethane	5.12	1936	1866	3.62
n-pentane	5.76	626	601	4.04
isopentane	5.78	620	598	3.61
n-hexane	6.01	659	637	3.39
cyclohexane	5.64	778	754	3.12
n-heptane	6.24	684	663	3.09
n-octane	6.46	702	682	2.84
isooctane	6.50	691	671	2.80
n-nonane	6.60	718	700	2.53
n-decane	6.86	731	713	2.47
n-dodecane	7.22	750	733	2.22
n-tetradecane	7.56	763	747	2.08
n-hexadecane	7.86	774	759	1.97
o-xylene	5.87	880	856	2.72
m-xylene	5.89	864	840	2.75
p-xylene	5.89	861	837	2.74
toluene	5.61	866	840	3.05
benzene	5.29	878	848	3.44
nitrobenzene	5.53	1206	1176	2.46
methyl alcohol	4.06	792	756	4.50
ethyl alcohol	4.59	790	760	3.86
n-propyl alcohol	4.99	804	779	3.09
isopropyl alcohol	5.03	786	762	3.05
n-butyl alcohol	5.34	810	788	2.72
isobutyl alcohol	5.35	802	780	2.74

where δ denotes the thickness of the surface layer, and the other symbols are as stated. Assuming — according to RUSANOV — that the thickness of the surface layer of the liquid is equal to the mean intermolecular distance d, calculated from formula (12a), we obtain the following expression for the density of the surface layer:

$$\varrho_1 = \varrho\left[1-\left(\frac{V}{N}\right)^{-1/3}\left(\frac{\partial\sigma}{\partial p}\right)_T\right]. \tag{19}$$

Table 2 gives densities of the surface layer of various liquids. It can be seen that the density of the surface layer of a liquid is several percent lower than the density of the liquid itself. For a number of homological saturated hydrocarbons this reduction decreases with an increasing homologue number, from 4.04 % for n-pentane to 1.97 % for hexadecane. A reduction in the value of the expression $(\varrho-\varrho_1)/\varrho$, with an increasing number of carbon atoms in the molecule, can also be observed for n-alcohols.

5. Conclusions

From the considerations presented in this paper the following conclusions can be drawn:

1. The coefficient K in Eötvös' formula, describing the dependence of the surface tension of a liquid on the temperature, is independent of the pressure unless the pressure is sufficiently high to change the packing structure of the molecules.

2. The formula derived in this paper, describing the pressure coefficient of the surface tension of a liquid, provides results which are in agreement with those obtained by other authors, e.g. SAHLI et al. [9]. SAHLI states that, in the case of carbon tetrachloride, the pressure coefficient of the surface tension begins to increase with increasing pressure no earlier than at a pressure of 2×10^6 [$\mathrm{Nm^{-2}}$]. This implies an evaluation of the limiting pressure, at which the packing structure of the molecules remains unchanged, on about 10^6 [$\mathrm{Nm^{-2}}$].

3. Formula (17) makes possible to evaluate the density of the surface layer of a liquid from the propagation velocity of ultrasonic waves in the liquid.

4. In a series of homological saturated hydrocarbons the value of the pressure coefficient of the surface tension $(\partial\sigma/\partial p)_T$ decreases with an increase of the homologue number. In the case of alcohols, it decreases with an increase in the number of carbon atoms in the molecule.

5. The density of the surface layer of a liquid is several percent lower than that of the liquid itself. In a homological series of saturated hydrocarbons, or of alcohols, the percentage reduction of the density of the surface layer, relative to the density of the liquid itself, decreases monotonically with an increase in the length of the chain which forms a molecule of a given compound.

References

[1] L. Brillouin, *Les tension superficielles; interpretation de la relation d'Eötvös*, Comptes Rendus, **180**, 1248–1253 (1925).

[2] R. V. Gopala Rao, *Phenomenological theory of surface tension and compressibility: evaluation of the parameter* τ, Ind. J. Pure Appl. Phys., **3**, 233–235 (1965).

[3] A. Kundt, *Über den Einfluss des Druckes auf Oberflächespannung an der gemeinschaftlichen Trennungsflache von Flüssigkeiten und Gasen und über die Beziehung dieses Einflusses zum Cagniard de la Tourschen Zustand der Flüssigkeiten*, Ann. Phys., **12**, 538–547 (1881).

[4] L. Landau, E. Lifszic, *Mechanics of continuous media*, [in Polish], PWN, Warszawa 1958, p. 297.

[5] Landolt-Börnstein, *Zahlenwerte und Funktionen aus Naturwissenschaften und Technik*, Gruppe 2, Band 5, Springer-Verlag, Berlin 1967.

[6] J. Partington, *An advanced treatise on physical chemistry*, Longmans Green, **2**, London 1955, p. 139.

[7] *Physico-chemical reference book* [in Polish], Wydawnictwa Naukowo-Techniczne, Warszawa 1974.

[8] A. I. Rusanov, N. N. Kotchzurova, W. N. Khabarov, *Issledowanije zawisimosti powierchnostnowo natjażenija żidkostej ot dawlenija*, Dokł. Akad. Nauk SSSR, **202**, 380–383 (1972).

[9] B. P. Sahli, H. Gager, A. J. Richard, *Ultracentifugal studies of the isothermal compressibilities of organic alcohols and alkanes. Correlation with surface tension*, J. Chem. Thermodynamics, **8**, 179–188 (1976).

[10] E. Słowiński, E. Gates, Ch. Waring, *The effect of pressure on the surface tension of liquids*, J. Phys. Chemistry, **61**, 808–816 (1957).

[11] E. Soczkiewicz, *Generalized Lennard-Jones potential and acoustic properties of liquids* [in Polish], Doctoral thesis, Institute of Fundamental Technological Research, Polish Academy of Sciences, Warszawa 1973.

Received on 9th December 1976

ARCHIVES OF ACOUSTICS
2, 3, 197-206 (1977)

TRANSVERSAL BLEUSTEIN-GULAYEV (B.G.) SURFACE WAVES ON A PIEZOELECTRIC CERAMIC

WINCENTY PAJEWSKI

Institute of Fundamental Technological Research, Polish Academy of Sciences (Warszawa)

In this paper the results of investigations of piezoelectric ceramic of the type lead zirconate-titanate (PZT) used as a basis for acoustic-electric waves (B.G.) are presented.

The inhomogeneous structure of the ceramic, which results from a particular technological process, was observed to influence the surface wave propagation. The ceramic structure, which causes velocity differences in the propagation velocity of an acoustic wave in the surface layers, can preclude the possibility of transversal surface wave propagation or can create more favourable conditions for its propagation depending on whether the volume wave velocity increases or decreases within the surface layers.

Investigations were carried out with plate and interdigital transducers for the generation of waves on the ceramic.

1. Introduction

Piezoelectric ceramic of the PZT type, is a material possessing good piezoelectric properties and is cheap and readily available. It has already found wide application in piezoelectric devices.

In view of the difficulties in obtaining suitable materials for acousto-electronic devices the idea emerged of using this piezoelectric ceramic as a basis for surface waves because of its characteristically large electromechanical coupling coefficient.

The currently produced ceramic has a basic fault, namely porosity. Porosity and graininess of the ceramic result from the technological process of its production. The obtained grain size (of the order of several or a dozen microns) constitutes an obstacle to the generation of elastic waves of high frequency. The discontinuity of the surface accounts for difficulties in polishing it suitably which is a basic condition for small surface waves attenuation at the higher frequencies.

Surface waves which are less sensitive to the surface condition are Bleustein-Gulayev (B.G.) waves which can penetrate quite deeply into the material.

Works on the utilization of the currently-produced ceramic (PZT) as a medium for surface waves [4] points to the possibility of using the ceramic at intermediate frequencies for colour television, and in delay lines at frequencies up to 30 MHz [5].

The technology of piezoelectric ceramics is constantly developing. Its properties are constantly being improved and this encourages the investigation into the generation and propagation of surface waves in ceramics. At present, only the conclusions drawn at lower frequencies are of a more general character, as results from the following pages of this paper.

2. Properties of Bleustein-Gulayev waves

A B.G. wave constitutes a special case of a LOVE wave which is propagating at the boundary of two media, in which molecules on the surface of the body and in its proximity are set into motion transversal to the direction of wave propagation. The motion of the molecules is related to the shear deformations in the plane of wave propagation. However, the conditions for the generation of B.G. waves are different from those for the generation of LOVE waves and are defined by the properties of the piezoelectric material.

B.G. waves can be considered to be a limiting state towards which a transversal volume wave moves under certain boundary conditions [1]. The properties of B.G. waves can be easily assessed with the aid of the relevant equations.

The propagation velocity of a B.G. wave at a free surface is described by the formula

$$v_s^2 = \frac{c}{\varrho}(1+k^2)\left[1-\left(\frac{1}{1+\varepsilon/\varepsilon_0}\,\frac{k^2}{1+k^2}\right)^2\right], \tag{1}$$

where c is the shear modulus, ϱ — the density of the material, ε_0 — the electric inductive capacity (permittivity) of the medium adjoining the air surface, ε — the electric inductive capacity of the material, and k — electromechanical coupling coefficient of the material.

In the case of a piezoelectric for which $\varepsilon/\varepsilon_0 = 730$, this velocity is very near to the velocity of the transversal wave expressed by the formula

$$v_T^2 = \frac{c}{\varrho}(1+k^2). \tag{2}$$

The velocity of the B.G. wave at a surface with a thin metallization layer and for which $\varepsilon_0 \to \infty$ and $1/(1+\varepsilon/\varepsilon_0) \to 1$ can be assumed, is given by

$$v_{sm}^2 = \frac{c}{\varrho}(1+k^2)\left[1-\frac{k^4}{(1+k^2)^2}\right] = \frac{c}{\varrho}\,\frac{1+2k^2}{1+k^2}. \tag{3}$$

It can be seen that the velocity of the B.G. wave at a metallized surface is smaller than the velocity of the transversal wave. For instance, for a piezoelectric ceramic with a coefficient $k = 0.5$ this velocity is $v_{sm} = 0.98v$, i.e. the difference in velocity is barely $2\,\%$. The penetration depth of the B.G. wave in the case of non-metallized surface is expressed by the formula

$$h = \frac{\lambda}{2\pi k^2}\left(1 + \frac{\varepsilon}{\varepsilon_0}\right). \tag{4}$$

In the case of a piezoelectric ceramic $\varepsilon/\varepsilon_0 = 730$, hence $k = 0.7$ and $h = 237\lambda$. Thus the B.G. surface wave is in this case very weak, all the elastic energy being bound with the transversal volume wave.

In the case of a metallized surface when $\varepsilon_0 \gg \varepsilon$, we have

$$h = \frac{\lambda}{2\pi k^2}, \qquad h = 0.64\lambda, \tag{5}$$

thus the larger part of the energy is concentrated in a surface layer 0.6λ thick.

The properties of acousto-electric waves can be utilized for investigating the structure of a piezoelectric ceramic. A necessary condition for the propagation of a transversal wave on the surface of a medium is that the velocity of the surface wave be smaller than the velocity of the transversal volume velocity. This condition is satisfied in the case of a piezoelectric ceramic when the ceramic is covered with a metallic layer which brings about a reduced rigidity of the surface layer by eliminating the internal electric field.

3. Methods of the generating acousto-electric waves in a ceramic

The generation of acousto-electric waves is quite a complicated problem, since along with the surface wave transversal and longitudinal bulk waves are generated. The isolation of the surface wave is thus complicated, especially in the case where the velocities of the transversal bulk wave and the surface wave are nearly the same.

The process of exciting a surface wave by means of a digital transducer, as is widely used, requires an especially selective transducer. Digital transducers with a large number of teeth meet such a requirement, but in practice this causes some difficulties. In the investigation of ceramics transducers with a smaller number of teeth or plate transducers can be used.

The latter are especially well-suited for the investigation of the properties of materials by means of surface waves. In order to excite surface waves using a plate transducer, it is sufficient to place at the side of the plate a transducer with transversal vibration and polarization parallel to the surface. It is a good practice for the transducer width to cover the thickness of the surface layer

in which the generation of waves occurs. This procedure for the generation of surface waves is of considerable practical importance, since owing to it we may avoid the laborious process of making digital transducers on the ceramic.

4. Experimental results

A digital transducer with four pairs of electrodes and an active tooth length of 4 mm, and also plate transducers, were used for the generation of B.G. surface waves. With the aid of two identical transducers a line, polarized

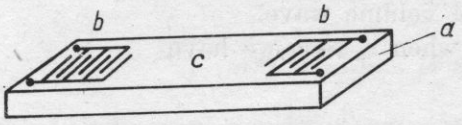

Fig. 1. Digital transducer on ceramic plate to be examined
a) plate of piezoelectric ceramic, *b*) transmitting and receiving transducer, *c*) metallized surface

vertically to the direction of the wave propagation and parallel to the plate surface, was constructed on the plate piezoelectric ceramic. The shape of the plate is shown in Fig. 1.

In the case under consideration the wave generation is related to the piezoelectric constant d_{15} which produces shear deformations under the action of an electric field.

The properties of transducers and lines were investigated using pulses of the order of microsecond with different carrier frequencies. At first, measurements were made on ceramic with a free surface and, secondly, with a metallized surface.

It results from the work of REDWOOD et al. [4] that in the case of a non-metallized surface the coupling of the surface wave is very weak and its penetration depth very large, so that practically only a transversal wave is generated in the thin plate.

Investigations performed with home-made ceramic, in which the direction of the pressure during pressing was vertical to the surface along which the wave was propagating, gave no positive results (Fig. 2).

Measurements of the transversal wave, generated by an interdigital transducer on plates with metallized and free surfaces, have not shown any essential differences. Indeed, in some cases the velocity of waves on the metallized specimens was higher than the velocity on the non-metallized ones (Fig. 2). Thus the necessary condition for the existence of transversal surface waves was not met.

For further investigations the specimen used were cut from round plates, made in such a manner that the direction of the pressure during pressing was parallel to the surface at which the surface wave was propagating.

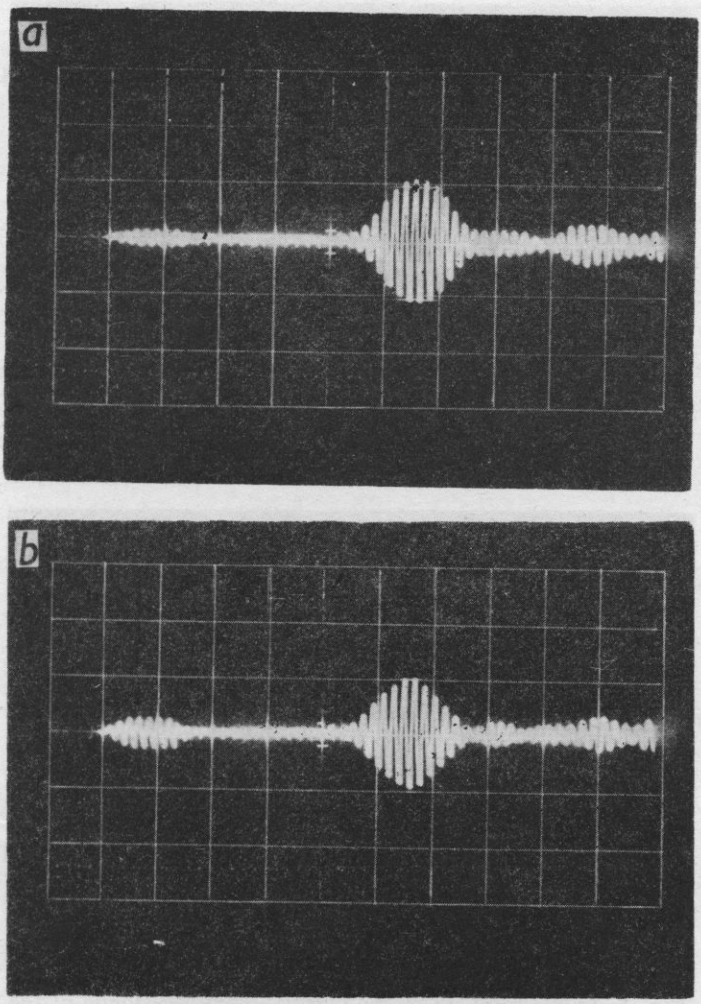

Fig. 2. Pulses received at the output of the line in Fig. 1
(f = 2870 MHz; 2 μs/div)
a) free surface v_s = 2380 m/s, *b*) metallized surface v_{sm} = 2380 m/s

Figures 3a, b show acoustic pulses generated and received on the surface of such a specimen by digital transducers at a frequency of approximately 2.5 MHz. Figure 3a shows pulses propagating along the free surface: the first impulse corresponds probably to the surface wave, the following ones to pulses reflected from the specimen ends. Figure 3b shows a surface wave on a metallized surface, in which case the reflections are weaker due to the bevelled edges of the specimen, while the increasing surface wave pulse can be seen early. From the difference of the wave velocities (Figs. 3a and 3b, Figs. 5a and 5b) it is possible to calculate the electromechanical coupling coefficient k_s according to the formula $k_s = v_s - v_{sm}/v_s$. In this case $k_s = 0.23$.

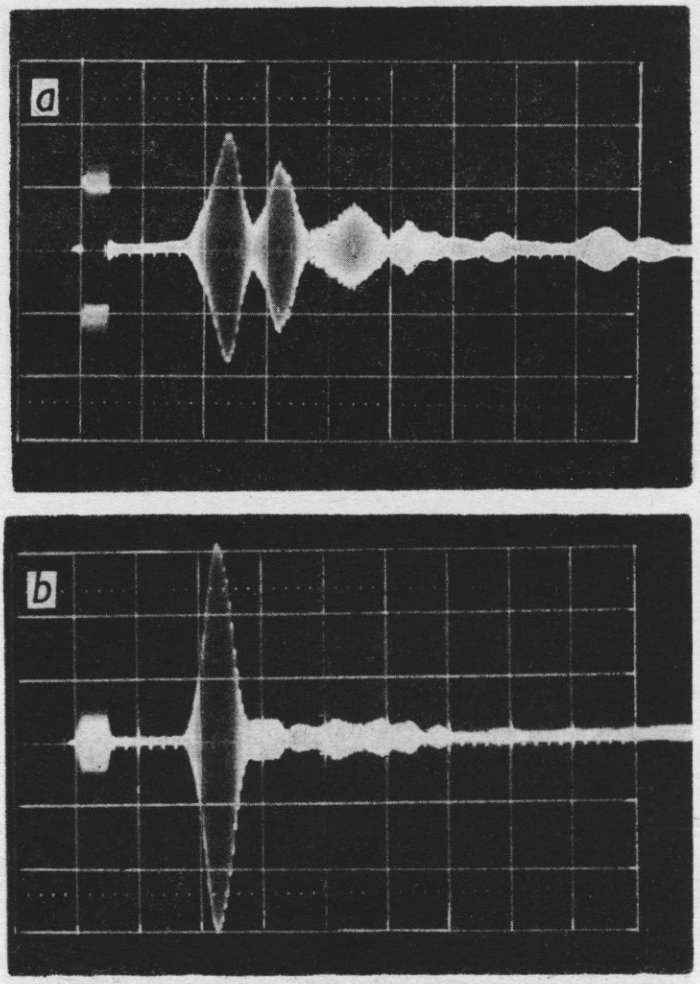

Fig. 3. Pulses received at the output of the line made of the ceramic plate (f = 2.5 MHz, 5 μs/div)
a) free surface v_s = 2380 m/s, *b*) metallized surface v_{sm} = 2320 m/s

The investigations of wave propagation on the non-metallized surface supported the suggestion that the first pulse in Fig. 3a is the one arising from the transversal surface wave. The thin metal coating on the surface causes a considerable increase in this pulse and reduces the wave velocity (Fig. 3b).

In order to identify more exactly the surface and transversal bulk waves, experiments were performed on large perpendicular parallelepiped of piezoelectric ceramic of foreign manufacture (Philips). Plate transducers, placed on side walls of the perpendicular parallelepiped (Fig. 4), were used for the generation of transversal surface wave.

Surface and bulk waves in the case of both metallized and free surfaces were investigated. For this purpose the transmitting transducer within the

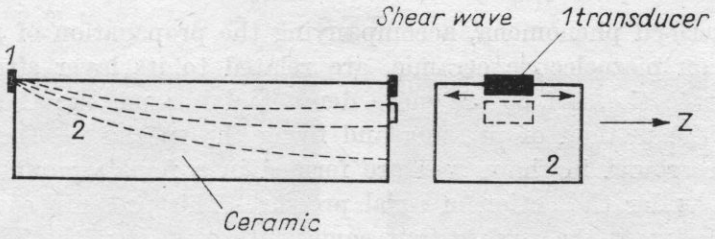

Fig. 4. Position of plate transducers for excitation of transversal surface wave
1 — transducer, *2* — ceramic to be examined

surface wave zone was immobilized, while the receiving transducer was moved away from the surface by 0.3, 1 and 2 mm. With such experiments evident differences were found in the image of the pulse at metallized and free surfaces.

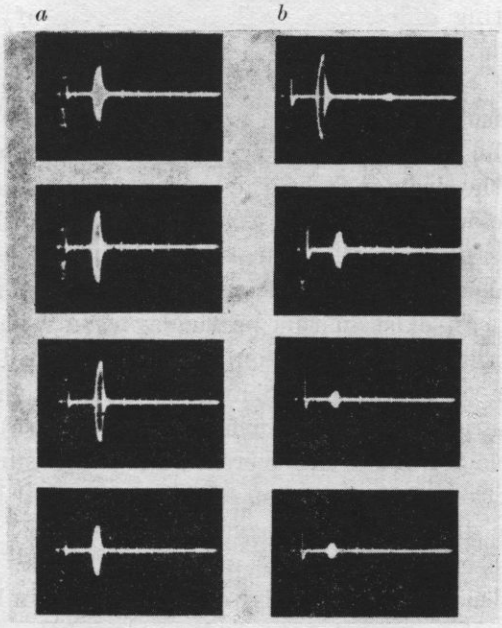

Fig. 5. Acoustic pulses excited by the plate transducers ($f = 5$ MHz, 5 μs/div)
a) free surface, receiving transducer placed at distances 0, 0.3 mm, 1 mm and 2 mm from the ceramic surface $v = 2440$ m/s, *b*) metallized surface, receiving transducer placed at distances 0, 0.3, 1 and 2 mm from the ceramic surface $v = 2380$ m/s

Figure 5a shows the image of the pulse at a free surface and Fig. 5b — at a metallized surface. In Fig. 5b it can be clearly seen that the decay of the received pulse as the transducer is shifted, while in Fig. 5a the pulse first increase and is observed to be followed by a decrease. The peak corresponds to an angle of about 20°.

The described phenomena, accompanying the propagation of surface and bulk waves on piezoelectric ceramic, are related to its layer structure. The layers nearer to the surface are more dense and less porous; their structure depends on the method of pressing and firing the specimens. Generally, the specimens are round in shape and are formed in a female mould of circular cross-section under the action of axial pressure. This pressure causes uneven compaction between the surface that comes into contact with the punch and the interior of the plate, caused by the inner friction of the ceramic composition. During firing the plate surface may have a higher temperature than the interior. This brings about a greater loss of lead from the surface layer and thus more intensive sintering. This process leads to an increased acoustic wave velocity in layers near to the surface and decreased velocity nearer the centre of the plate, the change being continuous. This property of the ceramic makes the generation and propagation of transversal surface waves difficult or even impossible. The coating of ceramic with a thin layer of metal and the subsequent decrease in the rigidity of the surface layer compensates only the higher rigidity of the layer because of inhomogeneous structure of ceramic. Consequently, the result is such as shown in Fig. 2.

In the case of the specimen shown in Fig. 3, the reverse phenomenon can be observed. Here the influence of the surface layers has been eliminated. Furthermore, the velocity of the transversal waves in the surface layer is smaller and increases towards the centre of the plate. Such conditions favour the generation of acoustic transversal surface wave with acousto-electric properties. Such waves can exist in this particular case without the plate being metallized. The metallization process only increases the difference in velocity between the interior of the specimen and its surface, thus considerably increasing the pulse amplitude of the surface wave (Fig. 5).

The changing velocity of the transversal wave at the surface of the specimen also affects the direction of propagation of the transversal bulk wave, by causing deflection of the direction of propagation of the bulk wave. This explains the behaviour of the transversal wave pulses in Fig. 5a.

REDWOOD has also foreseen a similar deflection, but in his paper the change in the velocity of the transversal wave in layers near the surface has occurred for the metallized surface and was caused by a change in ridigity modulus [4], resulting from the decay of the electric field.

The described phenomena and their explanation provide some possibility for the rational utilization of the structure of a piezoelectric material to improve the efficiency of the generation of transversal surface waves. With the present state of technology it is possible to utilize layers whose properties have already been determined.

Transversal waves with polarization vertical to the ceramic surface (thus to the axis z) were also generated by using plate transducers according to the arrangement shown in Fig. 6. It can be seen from the photographs that

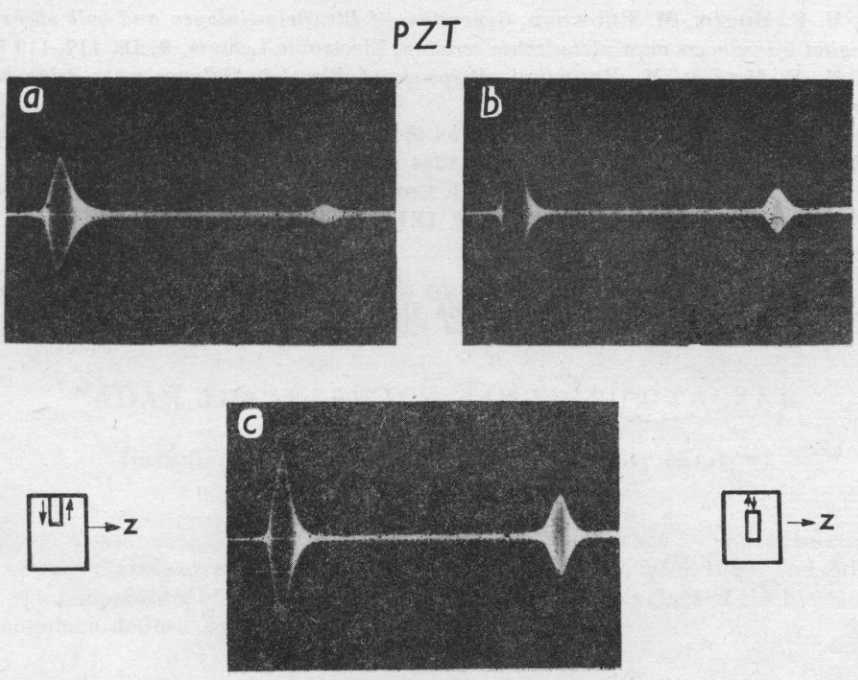

Fig. 6. Acoustic pulses on the piezoelectric ceramic when the transducer has a polarization vertical to the surface ($f = 2.358$ MHz, 2 μs/div)
a) transducers at a free surface $v_{T2} = 2170$ m/s, *b*) at a metallized surface $v_T = 2170$ m/s, *c*) transducers situated at the distance from the surface $v_T = 2170$ m/s

in this case no surface wave effects have been achieved. The velocity of waves beneath the surface and at the centre of the specimen was the same: 2170 m/s. The lack of the occurrence of surface waves (e.g. Rayleigh waves) was probably due to the irregular surface.

Similar experiments to those on ceramic were performed with crystals of lithium iodate on the x and y surfaces. As a result of the measurements made with plate, mean values of the coefficient k_s for ceramic and lithium iodate were determined:

piezoelectric ceramic (PZT): $k_s = 0.24$, $k = k_{15} = 0.56$;
lithium iodate LIO_3: $k_s = 0.3$, $k = k_{15} = 0.65$.

References

[1] C. A. A. J. Greebe, *Electromagnetic elastic and electroelastic waves*, Phil. Techn. Rev., **33**, 11–20 (1973).

[2] S. Kaliski, *Transversal surface wave in a piezosemiconducting body*, Bull. Acad. Pol. Sci., Ser. Sci. Techn., **18**, 69, 637 (1970).

[3] E. G. S. Paige, F. G. Marschall, *Novel acoustic surface wave directional coupler with diverse applications*, Electronics Letters, **7**, 460–462 (1971).

[4] M. F. Milson, M. Redwood, *Generation of Bleustein-Gulayev and bulk shear waves by interdigital transducers on a piezoelectric ceramic*, Electronic Letters, **9**, 18, 417–419 (1973).

[5] M. F. Milson, M. Redwood, *Response of Bleustein-Gulayev wave delay line on PZT-4 ceramic* (to be published).

[6] C. C. Tseng, *Elastic surface waves on the free surface and metallized surface of Cds, ZnO and PZT-4*, J. Appl. Phys., **38**, 4281–4284 (1967).

[7] W. R. Smith, H. M. Gerard, J. H. Collins, *Analysis of interdigital surface wave transducers by use of equivalent circuit model*, IEEE Tr. Microwaves Theor. Techn., **17**, 11 (1969).

Received on 20th December 1975

ARCHIVES OF ACOUSTICS
2, 3, 207-212 (1977)

INVESTIGATIONS OF THE HYDRATION OF POLYETHYLENEGLYCOLS USING AN ACOUSTIC METHOD

ADAM JUSZKIEWICZ, JADWIGA POTACZEK

Institute of Chemistry, Jagiellonian University (Kraków)

Measurements of the velocity of ultrasound in alcohol — water solutions of polyethylene glycols with molecular weights 400, 1500, 2000, 15000 and 20000 at a temperature of $25 \pm 0.1^{\circ}$C have been made and the values of the hydration numbers defined by the YASUNAGA method.

1. Introduction

The YASUNAGA method for the determination of hydration, is one of several known methods based on acoustic measurements. One of the first methods which subsequently provided the basis for further investigations was PASSYNSKY's method [1], with the aid of which it is possible to evaluate the hydration of electrolytes and non-electrolytes

$$h = \frac{(1-\beta/\beta_0)(1-g)}{g}, \tag{1}$$

where h is the hydration in terms of grams of solvent per gram of solute, β and β_0 are the adiabatic compressibilities of the solution and solvent respectively, and g is the number of grams of the solute dissolved in 1 gram of solution.

In deriving this expression, PASSYNSKY did not consider the compressibility of the solute. Such a simplification can only be valid for electrolyte solutions and for small solute concentrations.

An interesting modification of PASSYNSKY'S method was made by ERNST and JEŻOWSKA-TRZEBIATOWSKA [2] in the determination of the hydration numbers of some uranyl salts in an aqueous-organic mixture. To determine the hydration of uranyl sulphate and uranyl nitrate they used PASSYNSKY'S standard method while in the case of solutions of the same salts in a mixed water-dioxsan solvent they stated the following formula for the hydration

number:

$$n_h = \frac{c_1}{c_2} + \frac{c_3 \Phi k_3 - 10^3 \beta}{c_2 \overline{V}_1^0 \beta_1^0}, \tag{2}$$

where c_1, c_2, c_3 are the concentrations of water, electrolyte and dioxsan, respectively, in moles per 1 of solution, Φk_3 is the apparent molar compressibility of dioxsan in solution, β and β_1^0 are the adiabatic compressibilities of the solution and of water, respectively, and $\overline{V}_1^0$ is the volume of water.

Generally speaking, Φk_3 in this formula depends on the composition of the solvent and the concentration of the electrolyte, in order to determine these values and to evaluate the hydration numbers, use has been made of a special procedure involving the introduction of an organic constituent into the solution.

Another method of determining the hydration numbers was proposed by SHIIO [3, 4] using the dehydration properties of such liquids as ethyl alcohol or acetone.

The methods described above require a knowledge of the adiabatic compressibilities, and thus involves the necessity of the measuring both the sound velocity and the density of each solution.

In the method developed by YASUNAGA for the determination of hydration only the measurement of the velocity in the alcohol-water solutions is necessary. It is known that the dependence of the sound velocity on the alcohol concentration for alcohol-water mixtures is parabolic, its maximum being precisely defined for each temperature [5]. The addition of any substance causes a shift of the peak of the parabola in the direction of lower concentrations of alcohol. The difference between the abscissae of the maxima of the curves obtained is caused by the molecules of the solute bonding part of the water. With this assumption we have

$$\frac{A_0}{W_0} = \frac{A_1}{W_1 - W_x}, \tag{3}$$

where A_0 and W_0 are the amounts of alcohol and water corresponding to the maximum for alcohol-water mixtures without solute, A_1 and W_1 are amounts of alcohol and water at the maximum for alcohol-water solutions containing a certain amount of solute and W_x is the hydration in terms of percentage volume.

This paper presents measurements of the propagation velocity of ultrasound in alcohol-water solutions of polyethylene glycols with five different molecular weights over a range of concentrations from 1.4 g to 14.3 g per 100 g of water.

The investigations were aimed at determining the hydration of polyethylene glycols by YASUNAGA'S method and also the optimization of the con-

centration of macromolecules for which this method gives reproducible results. The investigations involved measurement of the propagation velocity of ultrasound using a "sing-around" method at a frequency of 10 MHz and at a temperature of $25 \pm 0.01°C$.

2. Experimental arrangement

All the materials used for the investigation of polyethylene glycol were made by BDH Chemicals Ltd. Measurements of the sound velocity as a function of ethanol concentration were performed for axis concentrations: 1.43, 2.86, 5.71, 8.57, 11.43, 14.29 g per 100 g of water for each polyglycol of the form

$$\begin{array}{l} CH_2-(CH_2-CH_2-O)_n-CH_2-OH. \\ | \\ OH \end{array}$$

Apparatus. The measurements of the sound velocity were made with the system shown in the block diagram of Fig. 1.

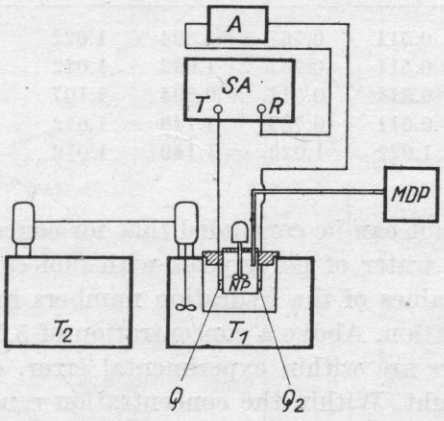

Fig. 1. Block diagram of the apparatus used for the measurement of the velocity of ultrasonic wave

A – ultrasonic wave velocity meter of the type SA 1000, developed by the Institute of Fundamental Technological Research, Polish Academy of Sciences, Warszawa, which enables a measurement of relative velocity to be made with an accuracy of up to 2 cm s, *A* – high frequency resistance attenuator, *MDP* – small-dimension metering pump, type 355 A developed by UNIPAN, Warszawa, which monitors the flow of ethanol into the measuring vessel with an accuracy of up to 0.02 ml, T_1 and T_2 – thermostat systems type NBE/NBER made in GDR, which ensure constant temperature in the measuring vessel with an accuracy of ± 0.01 °C, and *NP* – measuring vessel with agitator and transmitting and receiving transducers Q_1 and Q_2

3. Results and conclusions

Figure 2 shows the graph of ultrasonic velocity as a function of ethanol content for polyethylene glycol of molecular weights 400 and 20000, with a marked shift of the parabola in the direction of smaller ethanol concentration with increasing content of the substance examined.

On the basis of YASUNAGA'S formula

$$W_x = \frac{W_1 - A_1 W_0}{A_0}, \tag{4}$$

where W_x is the hydration for a certain amount of the substance examined, and the other symbols have the same meaning as in formula (3). The total hydration of all the polyglycols at six concentrations has been calculated and then converted into 1 g of solute.

Table 1 shows the values of the hydration numbers for polyglycols with molecular weights 400, 1500, 2000, 15000 and 20000 for concentrations ranging from 1.4 to 14.3 g per 100 g of water.

Table 1. Values of the hydration number (ml/g of dissolved substance)

Polyethylene glycol	c[g/100 g H_2O]					
	1.43	2.86	5.71	8.71	11.43	14.29
400	0.511	0.767	0.894	1.022	1.149	1.175
1500	0.511	0.767	1.022	1.022	1.149	1.124
2000	0.511	0.511	0.894	1.107	1.149	1.175
15000	0.511	0.767	1.149	1.022	1.149	1.226
20000	1.022	1.022	1.149	1.072	1.149	1.226

From these results it can be concluded that for concentrations in the range 1.4-5.7 g per 100 g of water of polyglycols with molecular weights 400, 1500, 2000 and 15000 the values of the hydration numbers increase with increasing of polyglycol concentration. Above a concentration of 5.7 g per 100 g of water, the hydration numbers are within experimental error, constant and independent of molecular weight. Within the concentration range 1.4-5.7 g per 100 g of water, the total amount of bound water determined from the shift of the parabola varies between 0.8-5 ml. The minimum dose of alcohol that causes perceptible changes in the shift of the maximum point of the parabola is 0.2 ml and this gives an equivalent amount of bound water of about 0.6 ml.

Thus, if the total amount of water bound per unit amount of solute is smaller than 6 ml, the determination error is higher than 10%, and the obtained results are barely trustworthy.

At concentrations of 1.4-5.7 g per 100 g of water the determination error considerably exceeds 10%, and at the lowest concentration examined is almost as high as 60%, so that the results obtained in this concentration range cannot be taken into consideration.

For confirmation of our conclusions, measurements of the time longitudinal relaxation time T_1 of water solutions of polyethylene glycols in the above-mentioned concentration range have been made in the Radiospectro-

scopy Establishment of the Physics Institute, Jagiellonian University, Kraków. The measurement were performed with a pulse spin echo apparatus, operating at a proton resonance frequency of 25 MHz by three method 180-90-180, at constant temperature of 22°C.

The relation between the longitudinal relaxation time T_1 for water solutions of macromolecules and their concentration is described by the linear equation [6, 7, 8, 9]

$$\frac{1}{T_1} = \frac{1}{T_{1w}} + kc, \tag{5}$$

where T_1 is the longitudinal relaxation time and T_{1w} the relaxation time of pure water, while the quantity k is proportional to the amount of water bound within the molecules of the solute.

The water found in the hydration envelopes of the macromolecules is less mobile than the free water which is not bound to the macromolecules.

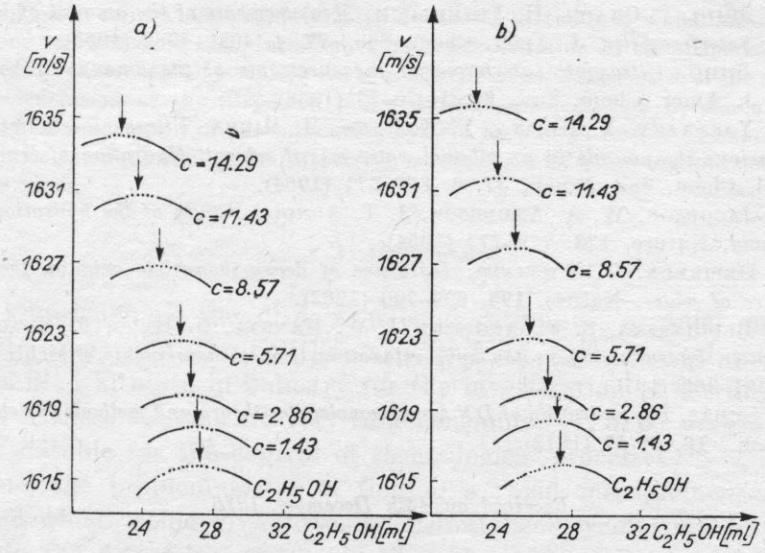

Fig. 2. Propagation velocity of ultrasonic waves as a function of ethanol concentration for ethylene polyglycol with molecular weight 400 and 20000

The relaxation process of the molecules of unbound water is therefore considerably faster than that of water bound within the molecules of the solute. When it is assumed that the interchange between molecules of free and bound water is very rapid, a shorter relaxation time for the solution in comparison with that of pure water can be observed.

The results for the longitudinal relaxation time T_1 for water solutions of polyethylene glycols with molecular weights 400, 1500, 2000, 15000 and 20000, over a concentration range from 4 to 10% by volume, have shown that the

relaxation time does not depend on the chain length of the polyethylene glycols tested. From this it results, in agreement with the results of the ultrasonic measurements, that the amount of bound water does not depend on the molecular weight of the polyethylene glycols, but only on their concentration in the solution.

*

This paper was partly financed by the U.S. Agricultural Dept. under Public Law 480 agreement.

References

[1] A. P. Passynsky, *Solvatacija nieelektrolitov i shimajemost ich rastvorov*, Żur. Fiz. Chim., **20**, 9, 981–994 (1946).

[2] S. Ernst, B. Jeżowska-Trzebiatowska, *Application of Passynsky's method for determination numbers of electrolytes in water-organic mixtures*, J. Phys. Chem., **79**, 20, 2113–2116 (1975).

[3] H. Shiio, T. Ogawa, H. Yoshihashi, *Measurements of the amount of bound water by ultrasonic interferometer*, J. Amer. Chem. Soc., **77**, 4. 4980–4982 (1955).

[4] H. Shiio, *Ultrasonic interferometer measurements of the amount of bound water. Saccharides*, J. Amer. Chem. Soc., **80**, 1, 70–73 (1958).

[5] T. Yasunaga, Y. Hirata, Y. Kawano, M. Miura, *Ultrasonic studies of the hydration of various compounds in an ethanol-water mixed solvent. Hydration of inorganic compounds*, Bull. Chem. Soc. Japan, **37**, 6, 867–871 (1964).

[6] B. Jacobson, W. A. Anderson, J. T. Arnold, *Study of the hydration of deoxyribonucleic acid*, Nature, **173**, 772–773 (1954).

[7] J. Depireux, D. Williams, *Influence of deoxyribonucleic acid on the intermolecular structure of water*, Nature, **195**, 699–700 (1962).

[8] B. Blicharska, Z. Florkowski, J. W. Hennel, G. Held, F. Noack, *Investigation of protein hydration by proton spin relaxation time measurements*, Biochim. Biophys. Acta, 207, 381–389 (1970).

[9] B. Lubas, *The hydration of DNA macromolecules-theory and methods of determination*, Post. Biochem., **18**, 31-57 (1972).

Received on 13th December 1976

ARCHIVES OF ACOUSTICS
2, 3, 213-224 (1977)

AN ACOUSTIC METHOD FOR THE DETERMINATION OF DISPERSIVECOMPOSITION OF ORGANIC SUSPENSIONS

STANISŁAW SZYMA

Institute of Physics, Silesian Technical University (Gliwice)

In this paper it is shown that the sedimentation analysis of an organic suspension can be made rapidly using ultrasonic methods in which an ultrasonic plane wave is used to induce very rapid sedimentation of the dispersed phase, while a transversal ultrasonic wave is used to determine the course of the changing concentration of the dispersed phase during sedimentation in the ultrasonic field. A description of the measuring system as well as results of experimental studies for determining the dispersive composition of some organic suspensions are given.

1. Introduction

A knowledge of the dispersive composition of organic suspensions is especially important during the inspection of technological processes. The methods used hitherto in industry for the investigation of the dispersive composition of these systems are very time-consuming [4, 5, 6], and for this reason are not suitable for the control of technological processes.

Thus, the problem arises of finding a rapid measurement method, i.e. a method which would give virtually instantaneously information on the conditions in the dispersive system as they change with time.

In this paper we show that the instantaneous condition of a dispersive system can be determined with the aid of an acoustic method by measuring the wave impedance of the tested dispersive system during the "settling" of molecules of the dispersed phase in an ultrasonic field.

2. "Settling" of molecules of the dispersed phase in the field of a plane acoustic wave

In initially considering the influence of an acoustic plane wave on the distribution of the concentration of molecules suspended in a dispersive system we shall assume the following:

(a) the molecules of the dispersed substance have spherical symmetry, with the molecule radius considerably smaller than the wavelength of the ultrasonic plane wave;

(b) the radii and masess of molecules of the dispersed phase and the dispersing substance satisfy the relations $r \gg r_0$ and $m \gg m_0$;

(c) the medium is considered to be lossless so that instantaneous velocities result only from the same wave conditions.

On the basis of these assumptions we can apply KING's [7] theory for solving the problem concerning the action of the acoustic radiation pressure on a sphere. According to this theory, in a sound wave propagating within the system a suspended spherical molecule is acted upon by the force. In the case of the plane wave this force is expressed by the formula

$$F = \pi g_0 |A|^2 \sin(2kx) \left\{ \frac{1}{aT_0T_1} - \frac{2[a^2 - 3(1-\varrho_0/\varrho_1)]}{a^5 T_1 T_2} + \right.$$
$$\left. + \frac{3(a^2-8)}{a^7 T_2 T_3} - \dots \right\}, \qquad (1)$$

where

$$a = kr, \quad k = \frac{2\pi}{\lambda}, \quad T_0 = a^{-1}, \quad T_1 = \frac{2+\varrho_0/\varrho_1}{a^3},$$

$$T_2 = 9a^{-5}, \quad T_3 = 60a^{-7}, \quad \dots, \quad T_n = \frac{1 \cdot 3 \dots (2n-1)(n+1)}{a^{2n+1}},$$

r denotes the molecular radius of the dispersed phase.

From expression (1) we obtain an approximate formula in the form

$$F = \pi g_0 |A|^2 \sin(2kx) a^3 \frac{1 + \frac{2}{3}(1 - g_0/g_1)}{2 + g_0/g_1} + R(a^i), \quad i = 4, 5, \dots, \qquad (1a)$$

where $R(a^i)$ denotes the remaining terms of a series containing the terms $z(a^4)$ and higher.

With the assumption that the molecular radius of the dispersed phase is considerably smaller than the ultrasonic wavelength ($a \ll 1$), it is possible to neglect the terms $z(a^4)$ and higher in formula (1a), whence we obtain

$$F = \pi g_0 |A|^2 \sin(2kx) a^3 \frac{1 + \frac{2}{3}(1 - g_0/g_1)}{2 + g_0/g_1}, \qquad (2)$$

where g_0 and g_1 denote the density of the dispersing and dispersed media, respectively.

As can be seen from formula (2), this force is equal to zero for the nodes and antinodes of the vibrations and attains its maximum between them. It can be easily proved that the direction of this force depends on the value of

relative density g_0/g_1 of the dispersed substance. Thus, for example, with a relative density of the molecules of the dispersed phase $g_0/g_1 < 2.5$, this force is directed towards the antinodes, whereas with a relative density of the molecules of $g_0/g_1 > 2.5$ it will be directed towards the nodes of vibration. This means that under the action of the wave pressure the molecules suspended in the medium will move – depending on the value of g_0/g_1 – towards the antinodes or nodes of vibration. Thus in the presence of a stationary plane wave in a dispersive system there is a change in the concentration distribution of the molecules of the dispersed phase. These conclusions have been confirmed by numerous experiments [3, 6, 7].

The phenomenon described above constitutes an analogue of gravitational sedimentation and therefore will in future be called *acoustic sedimentation.*

Let us first consider the process of acoustic sedimentation in a monodispersive system. Let us assume that the molecules suspended in the system move only under the action of the acoustic field, i.e. the dispersing medium is sufficiently viscous and the size of molecules of the dispersed phase sufficiently large. It is then possible to neglect the thermal and gravitational motion of these molecules. The equation of motion for one molecule suspended in the medium takes the form

$$6\pi\eta r\frac{dx}{dt} = \pi g_0|A|^2(kr)^3\sin(2kx)\frac{(5g_1-2g_0)}{(6g_1+3g_0)}, \tag{3}$$

where η denotes the viscosity of the dispersing medium, r – the molecular radius of the dispersed phase, $|A|$ – the amplitude of the acoustic potential, g_0 and g_1 – the densities of the dispersing and dispersed media, and x – the distance of a suspended molecule from the plane of an antinode.

Integrating this equation, we obtain

$$\tan(kx) = \tan(kx_0)e^{Bt}, \tag{4}$$

where

$$B = \frac{8\pi^2r^2\bar{E}(5g_1-2g_0)}{3\lambda^2\eta(6g_1+3g_0)},$$

and $\bar{E}$ denotes the acoustic energy density.

Let us further assume that the suspended molecules do not interact (λ is constant during the acoustic sedimentation) and initially are evenly distributed within the whole of the distributing system, so that the number of molecules suspended between planes x_0 and x_0+dx_0 is n_0dx_0, where n_0 denotes the concentration of molecules at $t = 0$. Then after a time t of the acoustic sedimentation the number of suspended molecules, contained between planes x and $x+dx$, is $n\,dx$, where n denotes the concentration of molecules after a time t of the process.

Under these conditions we have

$$n\,dx = n_0 dx_0. \tag{5}$$

According to equation (5) we find from formula (4) that the distribution of relative concentration (n/n_0) is given by the expression

$$\frac{n}{n_0} = \left(\cosh Bt - \cos(2kx)\sinh Bt\right)^{-1}. \tag{6}$$

Figure 1 shows the distribution of relative concentration of suspended molecules which hase been calculated for the case of a suspension consisting of dispersed particles of radius 1 μm, viscosity $\eta = 18.5$ cP, in an ultrasonic

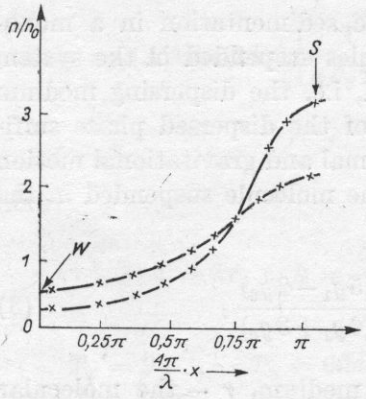

Fig. 1. Distribution of molecular concentration of the dispersed phase evaluated at times $t_1 = 210$ s and $t_2 = 430$ s during acoustic sedimentation

W and *S* denote the corresponding positions of a node and an antinode vibration

field of frequency 20 kHz and energy density 10^{-4} J/cm^3, at $t_1 = 210$ s and $t_2 = 430$ s.

The curves plotted in Fig. 1 for an ideal suspension show that at a small intensity of the ultrasonic field (about 2 W/cm^2) the molecules of the dispersed phase concentrate under the action of the wave pressure at the antinodes of the stationary ultrasonic wave. Substituting particular values into formula (6) it can be shown that in a plane x the concentration of molecules of the dispersed phase at the nodes decreases, but at the antinodes it increases exponentially with the duration of the acoustic sedimentation

$$n_w = n_0 e^{-Bt}, \tag{7a}$$

$$n_s = n_0 e^{Bt}, \tag{7b}$$

where n_w and n_s denote the concentrations of the molecules of the dispersed phase at the nodes and at the antinodes after a time t of the duration of the process.

From formulae (7a) and (7b) we obtain

$$n_w n_s = n_0^2. \tag{8}$$

This relation constitutes the characteristics of a dispersive system in which the sedimentation occurs under the influence of an ultrasonic field of plane stationary waves.

Let us now consider the process of acoustic sedimentation of molecules in a polydispersive suspension consisting of a certain number of different sizes of molecules of dispersed phase.

Using formula (6) and the assumption that the density of the dispersed molecules does not depend on their radius, the distribution of the volume concentration of the dispersed molecules in a polydispersive medium during acoustic sedimentation takes the form

$$\varphi_{x,t} = \sum \varphi_{0,i}(\cosh B_i t - \cos(2kx)\sinh B_i t)^{-1}, \tag{9}$$

where $\varphi_{x,t}$ denotes the volume concentration of dispersed molecules in the plane x at a time t, $\varphi_{0,i}$ is the volume concentration of the dispersed molecules of the i-th size at time $t = 0$, and

$$B_i = \frac{8\pi^2 \bar{E}(5g_1 - 2g_0)}{3\lambda^2 \eta(6g_1 + 3g_0)} r_i,$$

where r_i denotes the radius of a suspended molecule of the i-th size and $\bar{E}$ — the acoustic energy density.

From formula (9) it can be seen that the volume concentration of the dispersed molecules in a polydispersive suspension — as in the case of monodispersive system — decreases at the nodes of vibration, while at the antinodes it increases exponentially during the acoustic sedimentation process.

3. Analysis of acoustic sedimentation

When an organic suspension is polydispersive, the molecules of the individual fractions sediment under the influence of the field of plane stationary waves at different rates. Let us assume that the volume of molecules of the dispersed phase consists of volume fractions $\varphi_1, \varphi_2, \ldots$ corresponding to the radii $r_1, r_2, \ldots$ Then we can write

$$\varphi = \sum \varphi_i.$$

From formula (9), a change in the volume concentration caused by molecules wholly leaving the area, e.g. at a node of vibration, is

$$\Delta\varphi_{w,t} = \sum \varphi_{0,i}(1 - e^{-B_i T}), \tag{9a}$$

where $\varphi_{0,i}$ denotes the volume concentration of dispersed molecules of the i-th size at $t = 0$.

The change of volume concentration $\Delta\varphi_{w,t}$, brought about during the acoustic sedimentation, is determined by an ultrasonic transversal wave resonator [10, 11].

Using:

(a) the expression for the wave impedance of a medium

$$Z_L = R_L + iX_L, \tag{10}$$

(b) the relation between the viscous and elastic components of the wave impedance at a frequency $\omega \ll \omega_r$ [8]

$$R_L = X_L = (\pi f \eta_s g)^{1/2}, \tag{11}$$

(c) Einstein's law for the viscosity of a suspension

$$\eta_s = \eta_0(1 + b\varphi_{x,t}), \tag{12}$$

(d) the relation between the attenuation coefficient of an ultrasonic resonator and the wave impedance of the medium [9]

$$\alpha = k_0 Z_L, \tag{13}$$

we can derive a relationship between the volume fraction of dispersed molecules and the attenuation coefficient of the resonator in the form

$$\alpha_t^2 = \alpha_0^2(1 + b\varphi_{x,t}), \tag{14}$$

where α_t and α_0 denote the attenuation coefficients of the dispersive system and the dispersing substance, while $\varphi_{x,t}$ is the volume fraction of the dispersed molecules.

Hence, by measuring the attenuation coefficient of an ultrasonic resonator it is possible to determine experimentally the time dependence of the volume concentration of dispersed molecules in a particular region, e.g. at a node of vibration during acoustic sedimentation.

From expression (14) it is possible to change the volume concentration of dispersed molecules. In the region of a node of vibration it takes the form

$$\Delta\varphi_{w,t} = \overline{\Delta\alpha}_{w,t} b^{-1}, \tag{15}$$

where

$$\overline{\Delta\alpha}_{w,t} = \frac{\alpha_0^2 - \alpha_{w,t}^2}{\alpha_0^2}$$

denotes the change of the relative attenuation coefficient of the vibrations caused by a change in the volume concentration of the dispersed molecules due to some leaving the region of the node of vibration.

If we give further consideration to the fact that B_i is generally of the order of 10^{-4} and use expressions (9) and (15), it can be easily proved that the basic equation of acoustic sedimentation can be written in the following

manner:

$$\bar{\Delta a}_{w,t} = \bar{\Delta a}_{w,r} + \bar{\Delta a}_{w,2} = \bar{\Delta a}_{w,r} + t\frac{d(\bar{\Delta a}_{w,t})}{dt}. \tag{16}$$

It consists of the following components:

(a) changes of relative attenuation coefficient $\bar{\Delta a}_{w,r}$, contributed by the fraction of molecules with a radius larger than a certain value, which could leave wholly the region of the node of vibration, expressed in terms of the initial concentration of these fractions, and

(b) changes of relative attenuation coefficient $\bar{\Delta a}_{w,2}$ caused by the part of the molecular fractions with a radius smaller than the limiting value of the radius, which have left the volume under consideration.

This change is in the form of the product of the instantaneous derivative of the change of the relative attenuation coefficient caused by the acoustic sedimentation of all the molecules at a time t and the duration of this process up to the time t.

This equation is completely analogous to the expression representing the settlement curve in the analysis of gravitational sedimentation. Thus, in the analysis of acoustic sedimentation we can proceed further as in the gravitational sedimentation analysis to the transition from a settlement curve to a distribution curve. In order to determine the molecular distribution curve of the dispersed phase as a function of the radius, we evaluate the ratio $d(\bar{\Delta a}_{w,r})/dt$ for the molecules, which have left the region of the node of vibration

$$\frac{d(\bar{\Delta a}_{w,r})}{dr} = \frac{d(\bar{\Delta a}_{w,r})/dt}{dr/dt}. \tag{17}$$

The value of the ratio dr/dt can be found from the expression for the "settlement" time of all molecules of radius r or greater,

$$t = \frac{L}{r^2}, \tag{18}$$

where

$$L = \frac{3 \times 10^5 \lambda^2 \eta (6g_1 + 3g_0)}{8\pi^2 \bar{E}(5g_1 - 2g_0)}. \tag{19}$$

Using expression (18), we obtain

$$\frac{dr}{dt} = -\frac{1}{2}\sqrt{\frac{L}{t^3}} = -\frac{r}{2t}. \tag{20}$$

Substituting into equation (17) the values for $d(\bar{\Delta a}_{w,r})/dt$ and dr/dt, we have

$$\frac{d(\bar{\Delta a}_{w,r})}{dr} = \frac{2t^2}{r}\frac{d^2(\bar{\Delta a}_{w,t})}{dt^2}. \tag{21}$$

This equation expresses the separation of the molecules according to their size.

Figure 2 shows the dependence of $\bar{\Delta}a_{w,t}$ on time, obtained experimentally. When we draw the tangent to the curve at the point which corresponds to the time of acoustic sedimentation t, it will intersect the ordinate axis at a

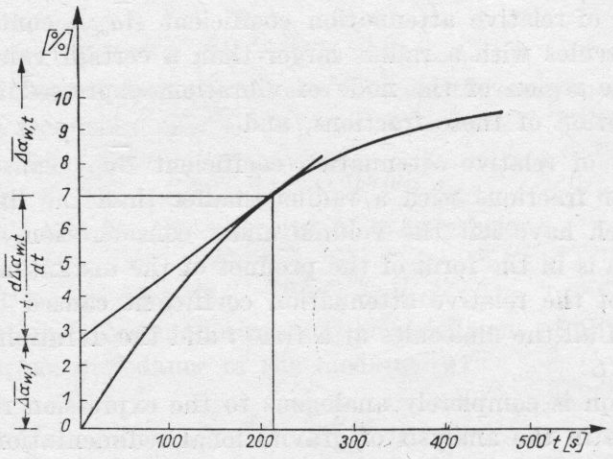

Fig. 2. "Settlement" curve of molecules of the dispersed phase at a node of vibration during acoustic sedimentation

certain value s which is equal to the change of the relative attenuation coefficient of the resonator $\bar{\Delta}a_{w,r}$ caused by the change of volume concentration of molecules with radius r and larger, which have left the region of the node of vibration after a time t, i.e.

$$s = \bar{\Delta}a_{w,r} = \bar{\Delta}a_{w,t} - t\,\frac{d(\bar{\Delta}a_{w,t})}{dt}.$$

Drawing a number of tangents to the curve at points corresponding to equal lengths of time, we can determine on the ordinate axis the differences in the lengths $\Delta(\bar{\Delta}a_{w,t})$. Since, however,

$$\frac{ds}{dr} = \frac{d(\bar{\Delta}a_{w,r})}{dr},$$

we can find, knowing $\Delta(\bar{\Delta}a_{w,r})$, the value of Δr. Thus, plotting r as the abscissa, we obtain the curve of molecular separation $[\Delta(\bar{\Delta}a_{w,r})/\Delta r]$.

4. Measuring system

Experimental investigations of acoustic sedimentation were performed with the measuring system shown in the block diagram in Fig. 3. The ultrasonic sedimentator consists of a source of ultrasonic plane waves, an electronic

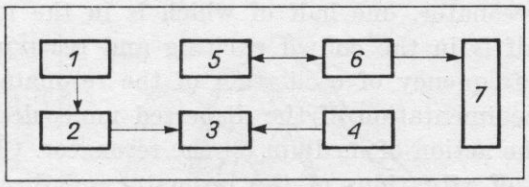

Fig. 3. Block diagram of the system for the measurement of acoustic sedimentation of the dispersed phase

1 – electric generator, *2* – magnetostrictive transducer with acoustic transformer, *3* – measurement vessel, *4* – ultrasonic wave reflector, *5* – sensor of measurement of the wave impedance of the tested system, *6* – system of excitation and reception of vibration, *7* – electronic system for the digital recording of measurement results

device for measurement of wave impedance of the suspension, an electronic system for digital recording, a thermostat and a measurement vessel with relatively rigid walls which effectively prevents the tested suspension from vibrating radially.

The ultrasonic generator is an electrical system with magnetostrictive transducer. The maximum power of the generator is 400 W and the transducer frequency is 20 kHz. The measurement vessel is formed as a brass cylinder of diameter 4 cm and height 10 cm. Over the measurement vessel there is the ultrasonic transducer with an acoustic transformer. Brass has been used for the construction of acoustic transformer. The lower part of the measurement vessel is a cylindrical reflector, its height corresponding to 5/4 of the ultrasonic wavelength in brass. The tranducer together with the acoustic transformer over the vessel can be shifted continuously by means of a screw. The cross-section of the measurement vessel is shown in Fig. 4. Vertically to the direction

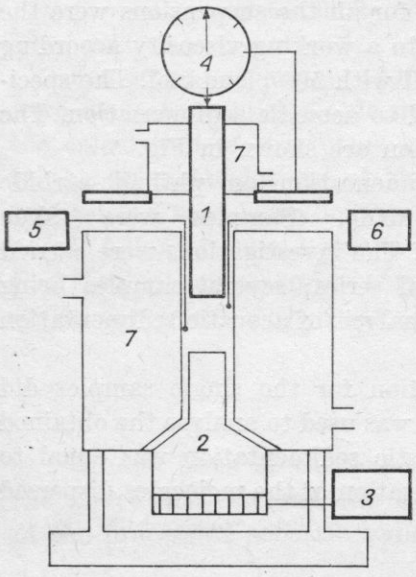

Fig. 4. Cross-section of measurement vessel of the acoustic sedimenter

1 – reflector, *2* – acoustic transformer, *3* – ultrasonic generator, *4* – sensor for measurement of the distance of the reflector from the source of the ultrasonic waves, *5* – thermistor thermometer, *6* – system for measurement of the wave impedance of the tested suspension, *7* – thermostat

of movement of the ultrasonic transversal wave there is placed the ultrasonic transversal wave resonator, one half of which is in the measurement vessel, while the other half is in the coil of exciting and receiving vibrations [11]. The characteristic frequency of oscillation of the resonator is 30 kHz.

The acoustic sedimentation of the dispersed molecules in the tested suspensions changes the action of medium on the resonator. Changes in the value of the attenuation of vibrations of the resonator are directly recorded by a digital printer.

5. Experimental procedure

In order to check the results of sections 2 and 3, investigation of dispersive composition using the above method were carried out on 2-component and polycomponent suspensions. The choice of the components and composition of the simple suspensions was decided by the composition and kind of the multicomponent organic suspensions to be tested.

Firstly, an analysis of acoustic sedimentation on 2-component suspensions with the following composition (designations of the composition according to standard PN – MPCH – 07) was made:

1 – suspension No 1 – 10%: 45/60% + titanium white,
2 – suspension No 2 – 10%: 45/60% + iron oxide red,
3 – suspension No 3 – 10%: 45/60% + poliogengelb RT 1560,
4 – suspension No 4 – 10%: 45/60% + monostral jast blue RFS.

These suspensions were prepared according to the following method: the pigment (in the ratio 1 : 1) has been mixed with resin mechanically and then ground in a disc mill. The grinding conditions for all the suspensions were the same. The suspensions obtained were thinned to a working viscosity according to Ford cup for 30 s in a solution melolak B/II with 50% budanol. The specimens, prepared in this manner, were subjected to acoustic sedimentation. The results of the analysis of acoustic sedimentation are shown in Fig. 5.

Secondly, the analysis of acoustic sedimentation on phthalic-carbide enamel (Manuf. No 3463-312-360) was made. (Samples were taken directly from the Paints and Lacquer Factory. The investigations were carried out on samples taken from various industrial series; several samples being prepared from each series. The results of the analysis of acoustic sedimentation of these samples are shown in Fig. 6.

The duration of the acoustic sedimentation for the single samples did not exceed 8 minutes. When a digital computer was used to analyse the obtained results, the time of the analysis of the acoustic sedimentation was equal to the duration of the process of acoustic sedimentation of the molecules dispersed in the suspension.

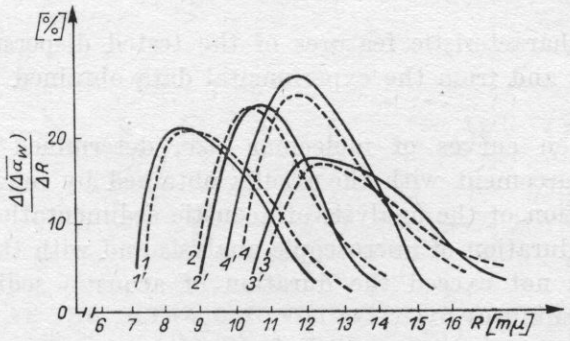

Fig. 5. Distribution of pigment molecules in suspensions *1, 2, 3, 4* according to their radius determined: a) by the acoustic method *1, 2, 3, 4*, b) by microscopy *1′, 2′, 3′, 4′*, with confidence limits for the determination of r of $\Delta r = \pm 0.5$ μm

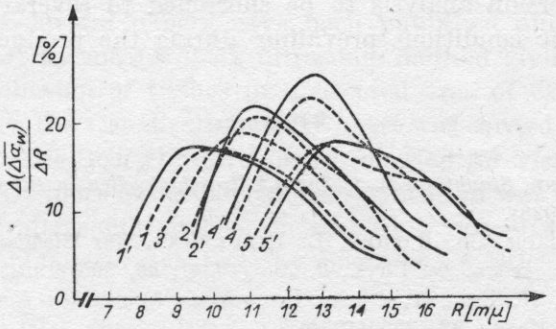

Fig. 6. Distribution of pigment molecules in enamel series *1, 2, 3, 4, 5* according to their size, determined by: a) the acoustic method *1, 2, 3, 4, 5* and b) microscopy *1′, 2′, 3′, 4′, 5′*, with confidence limits for the determination of r of $\Delta r = \pm 0.5$ μm

For some suspension additional investigations of dispersive composition were made by a microscopic method [5]. The preparation grain counting and the calculation of real value of grain distribution were performed according to the recommendations of the standard PN-70/C-04424. The results of investigations are shown in Figs. 5 and 6.

It follows from the results of the measurements presented in Figs. 5 and 6 that the distribution curves of molecule size, determined by the acoustic method, are in agreement with those obtained by microscopy.

6. Conclusions

On the basis of the experimental results obtained, it can be said that the above analysis and the conclusions resulting from it conveys a picture of the process of acoustic sedimentation, with the aid of which it is possible

to describe the characteristic features of the tested dispersive system. Thus from the analysis and from the experimental data obtained the following can be concluded:

(a) distribution curves of molecular size, determined by the acoustic method, are in agreement with the results obtained by microscopy;

(b) the duration of the analysis of acoustic sedimentation is considerably shorter than the duration of microscopic analysis and with the use of a digital computer it does not exceed the duration of acoustic sedimentation which lasts only a few minutes;

(c) it can be said, moreover, that the dispersive compositions of enamel samples from various industrial series are different.

From the above it can be seen that the acoustic method, described for the determination of the dispersive composition of organic suspensions, can be used during the inspection of technological processes, since it permits the time of the dispersion analysis to be shortened to several minutes and this corresponds to the conditions prevailing during the production.

References

[1] M. Ardenne, *Staubfiguren stehender Ultraschallwellen in Flüssigkeiten*, Funktechn. Monatshefte, 248 (1938).

[2] H. R. Asbach, Ch. Bashen, L. Hiedemann, *Zur Sichtbarmachung von Ultraschallwellen in Flüssigkeiten*, Zs. Phys., **8**, 738 (1934); **88**, 395 (1934).

[3] O. Brant, H. Freunt, *Einige Versuche in kundtschen Rohren mit Schallwellen hoher Frequenz*, Zs. Phys., 92, 385 (1934).

[4] M. J. Golden, *Microscops method for observing pigment dispersions*, J. Paint. Techn., 45, 54 (1973).

[5] Polish standard, *Pigments. Investigations of disintegration*, PN-70/C-4424.

[6] R. Hong, *Einige Aspekte der Teilschengressenbestimmung von Pigmenten durch Sedimentation in zentrifugal Feld*, Deutsch. Farb. Z. H., **2**, 59 (1171).

[7] L. V. King, *On the acoustic radiation pressure on spheres*, Proc. Rey. Soc., A **147**, 212 (1934).

[8] W. B. Mason, N. J. Murray Hill, *Measurement of the viscosity and shear elasticity of liquids by means of a torsionally vibrating cristal*, Trans. ASME, 5359 (1947).

[9] W. Rath, S. R. Rich, *A new method for continuous viscosity measurement, General theory of the ultra-viscoson*, J. Appl. Phys., **24**, 940 (1953).

[10] S. Szyma, *Über eine akustische Methode in der Lack- und Farbenindustrie*, Proceedings of 7th International Congress on Acoustics, **2**, 124, Budapest 1971.

[11] S. Szyma, *New type of ultrasonic viscosimeter*, Proceedings of 5th National Conference of Metrology and Construction of Measuring Devices, **5**, 114, Poznań 1972.

Received on 15th October 1976

ARCHIVES OF ACOUSTICS
2, 3, 225-230 (1977)

TECHNICAL WORKS

ATTEMPTS AT THE ULTRASONIC VISUALIZATION OF THE HEART IN REAL TIME

LESZEK FILIPCZYŃSKI, JAN SAŁKOWSKI

Institute of Fundamental Technological Research, Polish Academy of Sciences (Warszawa)

In recent years several papers have been published aimed at the visualization of the heart by means of an ultrasonic method giving a geometrical picture of the distribution of tissues in a selected area of examination.

The first work on the visualization of the heart was carried out by KIKUCHI [5] but it was not until BOM [1] developed a method for visualization of the heart in real time that more extensive clinical application was found (Fig. 1, I).

The pioneer of ultrasonic analysis in real time was SOMER [6] who was the first to examine biological structures by means of a multielement transducer

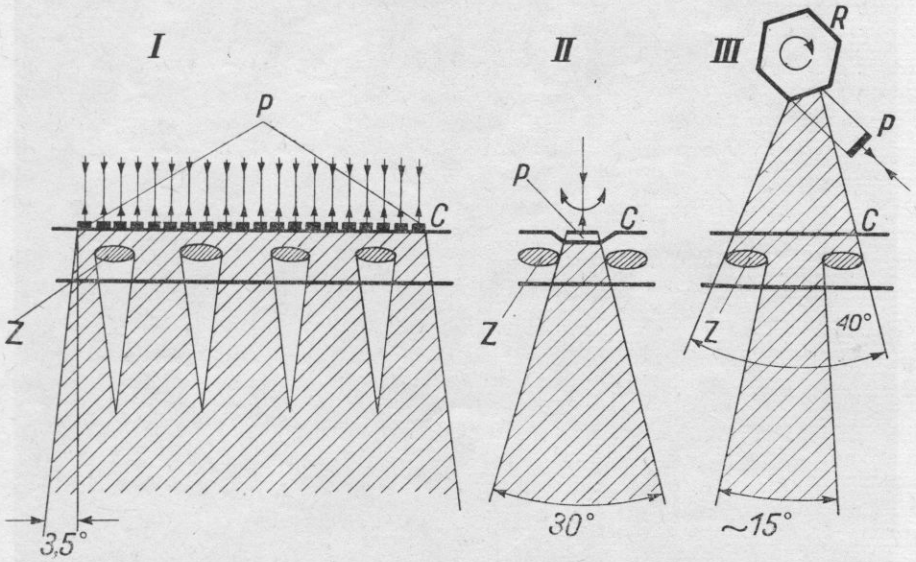

Fig. 1. Various methods of ultrasonic visualization of the heart in real time: *I* – with a transducer array [1, 7], *II* – with one oscillating transducer [2, 4], *III* – with one revolving reflector (IPPT-PAN)

P – piezoelectric transducers, *C* – body surface, *Z* – ribs, *R* – revolving reflector

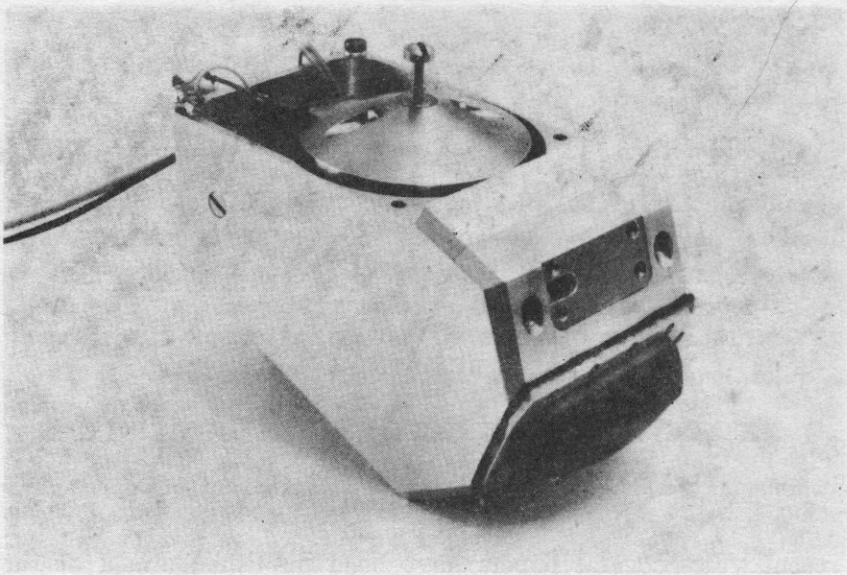

Fig. 2. Ultrasonic scanner (overall dimensions 130 × 80 × 75 mm) with a revolving reflector as shown in Fig. 1, *III*

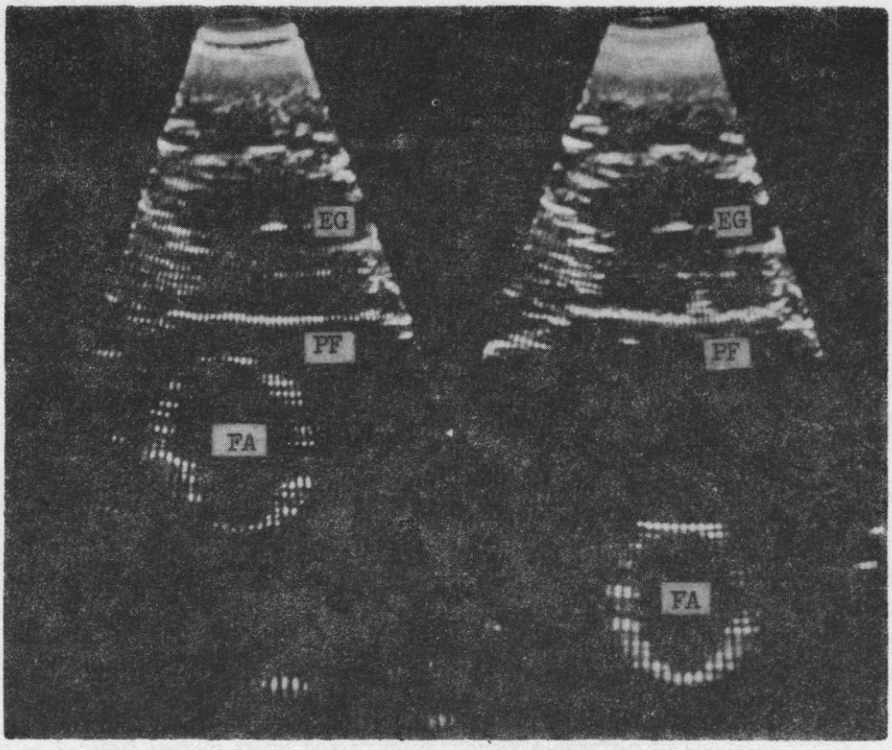

Fig. 3. Results of experimental investigations with an aorta phantom (*FA*) in various positions immersed in a tank containing water obtained with the system shown in Fig. 1, *III*

in which all transducers were excited simultaneously with voltages of variable phase.

A further improvement of such a system is that of THURSTONE [7], in which a multielement transducer array is controlled digitally by means of a special programme.

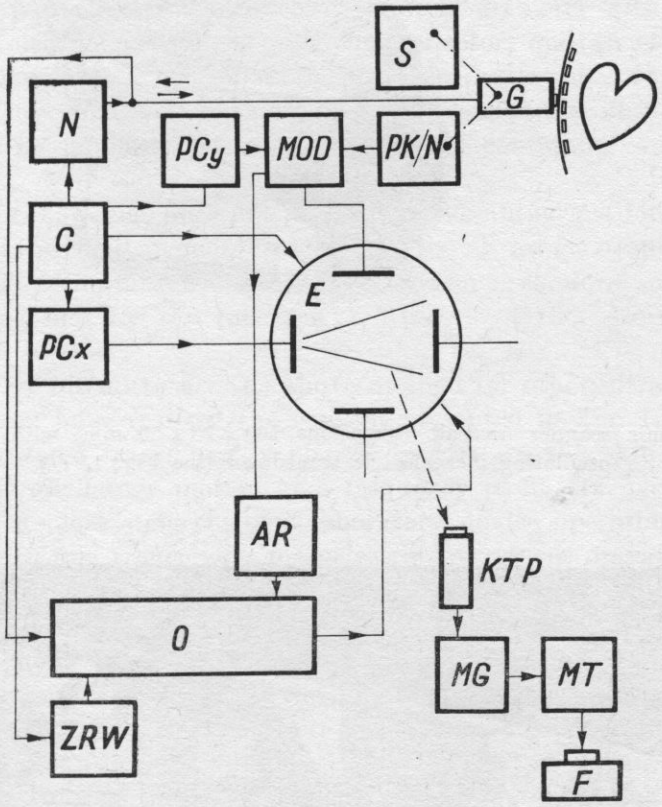

Fig. 4. Simplified block diagram of laboratory system for ultrasonic heart visualization in real time

C – timer, *PCx* – horizontal time base, *N* – transmitter, *G* – scanner with ultrasonic transducer, *S* – motor with transmission gear, *PK/N* – angle/voltage transducer, *O* – electronic receiver, *E* – oscilloscope screen, *PCy* – vertical time base, *MOD* – modulator, *AR* – automatic brightness system, *ZRW* – sensitivity-time control (swept gain), *KTP* – industrial TV-camera, *MG* – video-recorder, *MT* – TV-monitor, *F* – photographic apparatus

A different concept was proposed by GRIFFITH and HENRY [4] (Fig. 1, II) and EGGLETON et al. [2] with a single mechanically oscillating transducer. A similar concept has recently been realized by WHEATLEY [8].

In the Department of Ultrasonics of the Institute of Fundamental Technological Research of the Polish Academy of Sciences a method of ultrasonic

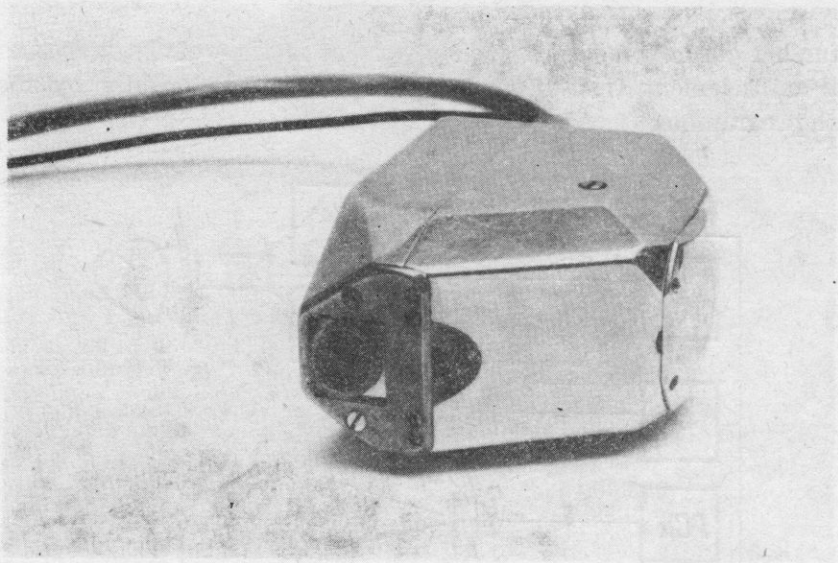

Fig. 5. Ultrasonic scanner (overall dimensions $100 \times 75 \times 50$ mm) with a mechanically oscillating piezoelectric transducer (see Fig. 1, *II*)

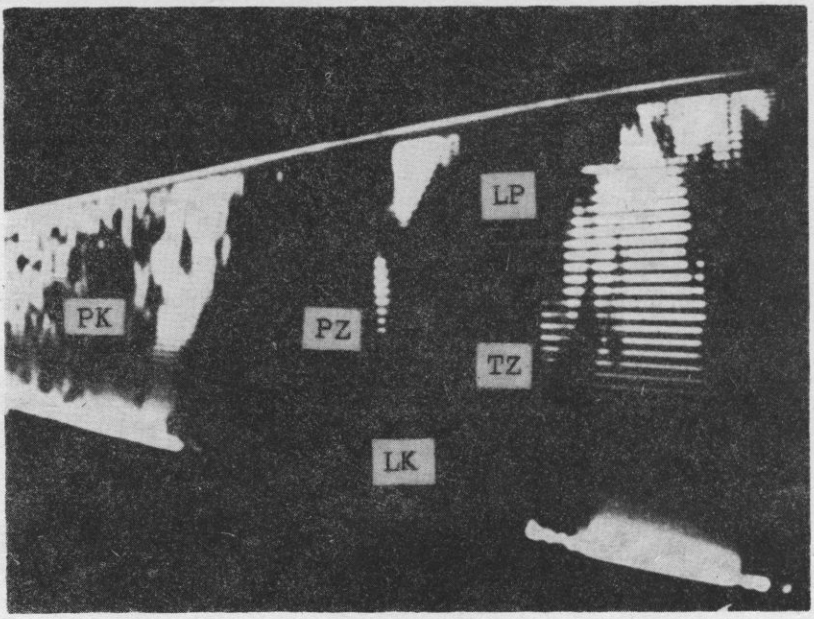

Fig. 6. Ultrasonogram of the heart obtained in real time

PK – right ventricle, *LK* – left ventricle, *LP* – left atrium, *PZ* – anterior leaflet of the mitral valve, *TZ* – posterior leaflet of the mitral valve

visualization has been proposed (Fig. 1, III), in which the ultrasonic beam makes unidirectional angular sweeps at a constant angular speed. This is achieved by using a reflector in the form of a prism with a regular hexagonal base revolving at a constant speed of about 5 revolutions per second. The reflector is immersed in a liquid container the bottom of which is a thin foil for coupling to the patient's body. The ultrasonic scanner is presented in Fig. 2. The scanner incorporates a piezoelectric transducer 10 mm in diameter with a frequency of 3 MHz, an electric motor, the revolving reflector, and an electrical pulse generating system which synchronizes the other electronic units of the apparatus. The results of investigations using this system (carried out on a model made of thin rubber to simulate the aorta) in a vessel containing water is shown in Fig. 3.

The system, however, does not seem to be advantageous for cardiological uses, because of the small angle interrogated by the ultrasonic beam — about 15° (Fig. 1, III). This limitation is caused by ultrasonic shadows of ribs for the frequencies used and by the (necessary) distance of the resolving reflector from the body surface.

Therefore we intend to use the above method for other ultrasonic diagnostic purposes and have realized the concept presented in Fig. 1, II [2, 4], in which the ultrasonic transducer is placed directly on the skin between the ribs and makes oscillatory motion at a frequency of 25 Hz.

A simplified block diagram of a laboratory device operating in a pulse-echo mode, with one tranceiving piezoelectric transducer operating at a frequency of 3 MHz and with a repetition frequency of 2 kHz, is presented in Fig. 4. Fig. 5 shows the ultrasonic scanner with the piezoelectric transducer visible. Fig. 6 shows the first result of heart examination. The right ventricle, the left atrium and ventricle and the posterior and anterior leaflets of the mitral valve can be seen.

In order to obtain full investigational results it is necessary to record the heart structure in motion. This has been done with an industrial TV-camera and a video-recorder permitting repeated observation of the heart structure in motion on a TV-monitor in addition to classical photographic documentation.

The report should be viewed as a preliminary one. Further work will necessarily involve the determination of the resolution of the method, the fidelity of reproduction of the anatomical structures, the optimization of these parameters, the investigation of the range of application of this method and the development of a method of synchronizing photographic documentation with electrocardiographic recording as this is necessary for clinical tests.

Nevertheless, the results obtained imply the conclusion that ultrasonic heart visualization in real time will soon become a clinical tool of great diagnostic significance in cardiology.

References

[1] N. Bom, *New concepts in echocardiography*, Stenfert Kroesse, Leiden 1972.

[2] Eggleton et al., *Visualization of cardiac dynamics with real time B-mode ultrasonic scanner*, In: "Ultrasound in medicine", Ed. D. White, **1** (1975).

[3] J. Etienne, L. Filipczyński, K. Ilmurzyńska, J. Sałkowski, *Ultrasonic investigation methods of heart function in obstetrics and cardiology* [in Polish], Archiwum Akustyki, **5**, 1, 113–128 (1970).

[4] J. Griffith, W. Henry, *A sector scanner for real time two-dimensional echocardiography*, Circulation, **XLIX**, 1147–1152 (1974).

[5] Y. Kikuchi et al., *Ultrasono-tomo-kymography of the heart*, Ultrason. Med., Ed. Bock et al., Wien. Med. Akad. 1969, 481–487.

[6] J. C. Somer, *Electronic sector scanning for ultrasonic diagnosis*, Ultrasonics, **6**, 2, 153 (1968).

[7] F. L. Thurstone et al., *Development of a real-time two-dimensional B-scan system using a phased transducer array*, 2nd Europ. Congr. Ultrason. in Med., München 1975, Abstracts of Papers, p. 66.

[8] D. J. Wheatley et al., *Cardiological applications of a new real-time ultrasonic sector scanner*, Digest of the 11th Intern. Conf. on Med. and Biol. Eng., 108–109, Ottawa 1976.

Received on 29th December 1976

C H R O N I C L E

VI WINTER SCHOOL OF MOLECULAR, QUANTUM ACOUSTICS AND HYDROACOUSTICS AND ULTRASOUNDS

Szczyrk, March 1977

VI Winter School of Molecular, Quantum Acoustics and Hydroacoustics and Ultrasounds was hold between 8-14 March at Szczyrk. The promotor of the Winter School was the Institute of Physics of Silesian University in Gliwice and the newly organized Section of Molecular and Quantum Acoustics attached to the Upper Silesian Department of the Polish Society of Acoustics (PTA). The Chairman of Organizing Committee was dr Stanisław Szyma.

The School was attended by over 30 participants from 10 scientific centres. In course of the School six sessions were held at which 27 lectures and reports were delivered giving a general review of the research work in Poland in quantum acoustics, acoustoelectronics, ultrasonic spectroscopy, hydroacoustics and ultrasounds.

List of lectures in their sequence of delivery

1. Session

J Zabawa, A. Klimasek, *Determination of the modulus of elasticity of anisotropic plates with cubic symmetry.*

J Berdowski, *Influence of isotropic effects on acousto-optical and dielectric properties of DADA crystals.*

Z. Kubik, A. Opilski, *The action of an elastic surface wave on free charge carriers in a semi-conductor-layer-piezoelectric system.*

Z. Cerowski, J. Grochowska, *Measurements of the wave propagation velocity by a resonance method in TgS and its dependence on crystallographic directions.*

2 Session

M. M. Dobrzański, *The representation of a hypersonic wave as a coherent macroscopic quantum condition.*

L. Lipiński, *Stochastic model of the stimulated ultrasonic low-temperature relaxation of stress in polycrystals.*

C. Lewa, *Piezoelectric properties of polymers.*

S. Śliwiński, *Effect of selective extinction of strias in the process of bending high-power light with ultrasound.*

P. Kwiek, *Holographic investigations of an ultrasonic field.*

Z. Toczyski, *Measurement of amplitude in ultrasonic waveguides used for the insonification of liquid media.*

3. Session

M. Szustakowski, *Light diffraction by acoustic surface waves.*

A. Byszewski, *Utilization of the acoustic stroboscopic effect for the visualization and investigation of vibrations in liquids and solids.*

I. MERTA, *Light diffraction by acoustic waves in an isotropic medium, considering terms of order* Δu^2.

W. PAJEWSKI, *Certain properties of transversel surface waves.*

Z. JAGODZIŃSKI, *Calibration of ultrasonic transducers.*

J. FINAK, A. KRZESIŃSKI, A. RAWICZ, *ZnO-layers for acousto-optics obtained by direct-current cathode dispersion.*

4. Session

B. ZAPIÓR, *Conditions for the correct interpretation of the effect of the action of ultrasound on liquid systems.*

L. WERBLAN, S. SKUBISZAK, *Some problems related to the measurement of the absorption and group velocity of ultrasonic in liquid media.*

S. SZYMA, *Acousto-electric method for the determination of the stability of physical properties of organic suspensions.*

5. Session

E. SOCZKIEWICZ, *The dependence of the surface tension of a liquid on the pressure and the radius of molecules.*

J. ZWIERNIK, *Sound velocity in overheated steam.*

Z. JAGODZIŃSKI, *Compression of pulses in ultrasonic echo-location systems.*

M. ALEKSIEJUK, *Generation and detection of acoustic vibrations at gigahertz frequencies using a Josephson joint.*

6. Session

S. PIEKARSKI, *The acousto-electric effect.*

Z. CEROWSKI, *The influence of a transversal field on surface wave propagation on a semiconductor-piezoelectric boundary.*

Taking advantage of the presence of interested persons on the 3rd day of the School, the Board of Quantum and Molecular Acoustics of PTA convened a general meeting at which 31 persons participated. At the meeting the board of the section was presented comprising: Chairman – A. OPILSKI (Institute of Physics of Silesian Technical University, Gliwice), Assistant Chairman – A. ŚLIWIŃSKI (Institute of Physics of Gdańsk University), Secretary – J. GRZYMEK (Institute of Physics of Silesian Technical University, Gliwice), Members – F. KUCZERA (Institute of Physics of Silesian Technical University, Gliwice) and M. M. DOBRZAŃSKI (Institute of Fundamental Technological Research, Polish Academy of Sciences).

The participants of the meeting were also informed of the Statute of the Section, approved by the Main Board of the PTA in November, 1976. Tasks facing the Section AMK were also discussed and it was suggested that the yearly Winter School of Molecular, Quantum Acoustics and Hydroacoustics and Ultrasounds be use for the coordinate and essential appruisal of scientific research work conducted in the subject of "Quantum acoustics and acoustoelectronics" and also "Ultrasonic spectroscopy", being interministerial problem MR. I. 24.

According to the opinion of participants, VI Winter School was of a good scientific level, and the warm and cordial atmosphere, created by the Organizing Committee, contributed to the establishment of close scientific contacts and exchange of views.

M. M. Dobrzański (*Warszawa*)